



XXVI International Workshop on Deep-Inelastic Scattering and Related Topics
16-20 April 2018
Kobe, Japan

Subnuclear fluctuations in vector meson photoproduction: a window to saturation

J. G. Contreras
Czech Technical University

In collaboration with Jan Čepila,
Michal Křelina and Daniel Tapia Takaki

April 18, 2018, Kobe

Work partially supported by grants 18-07880S (GAČR-CZ), LTC17038 (MŠMT, ČR), Conicyt PIA/ACT 1406 (Chile), Conicyt PIA/Basal FB0821 (Chile).

Contents and bottom line

- News from J/ψ production in γp collisions:
 - The energy dependence of dissociative J/ψ photoproduction provides a striking signature for saturation.
- News from J/ψ production in γPb collisions:
 - Fluctuations of subnuclear degrees of freedom also leave an imprint in the photoproduction of J/ψ off nuclear targets.
- News from other vector mesons:
 - The mass dependence of vector meson photoproduction provides a new handle in the search for saturation effects.

Čepila, JGC, Tapia , PLB 766 (2017) 186

Čepila, JGC, Křelina, PRC 97 (2018), 024901

Čepila, JGC, Křelina, Tapia, arXiv 1804.05508

Introduction

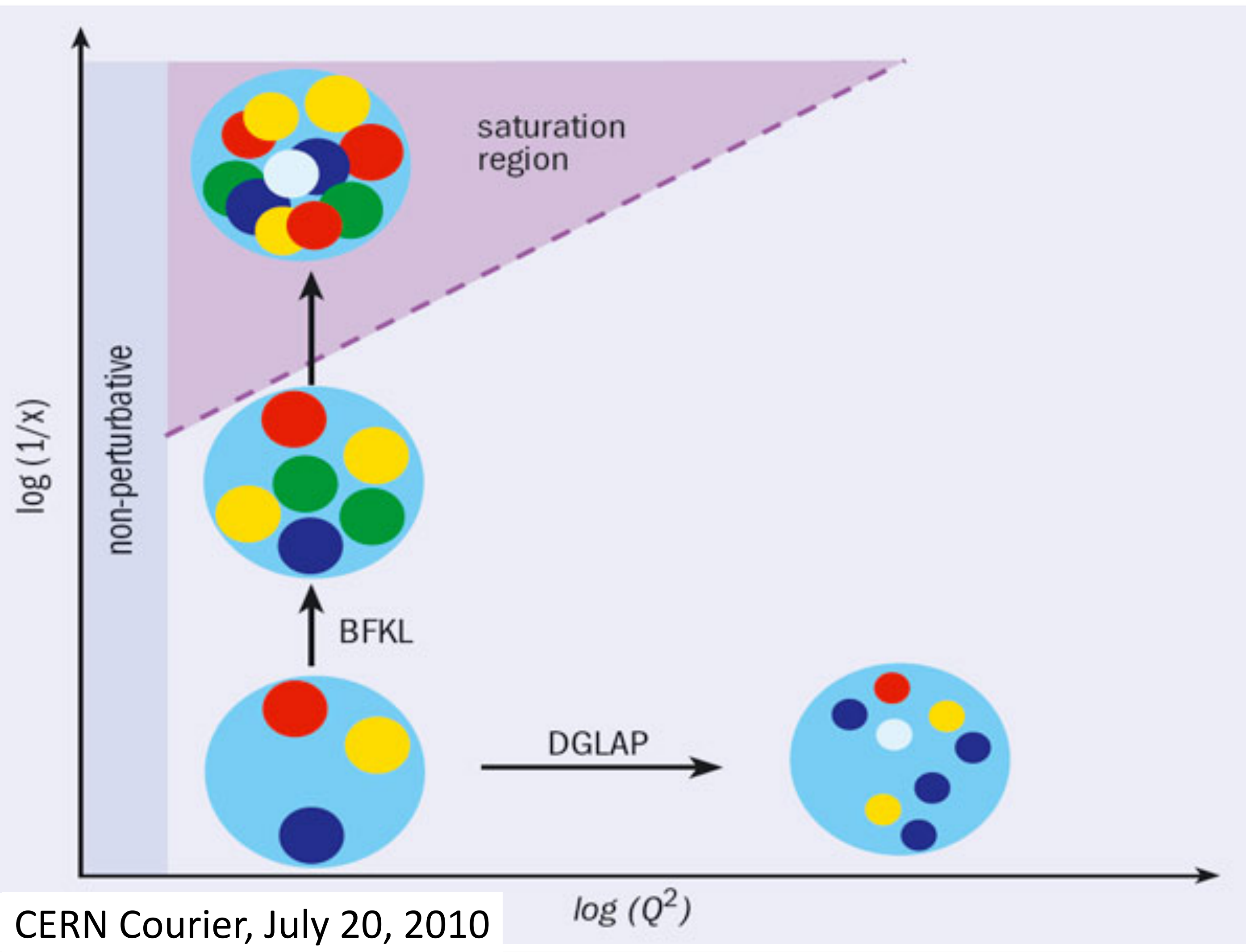
Introduction

See Heikki's talk on Monday!

- Fluctuations of subnuclear degrees of freedom in the impact-parameter plane, may yield signatures of saturation.
- Full formal treatment of this problem is difficult.
 - From the theory side there are open problems; e.g., how to deal with contribution from large dipoles.
 - The calculations need sizeable computational resources.
- Try to extract the main broad behaviour in a simple model.
 - Simple, but guided by pQCD.
 - Parameters, with reasonable values, fixed by as little data as possible to have some predictive power.
 - Agreement with data is comforting, but should not be overemphasised,

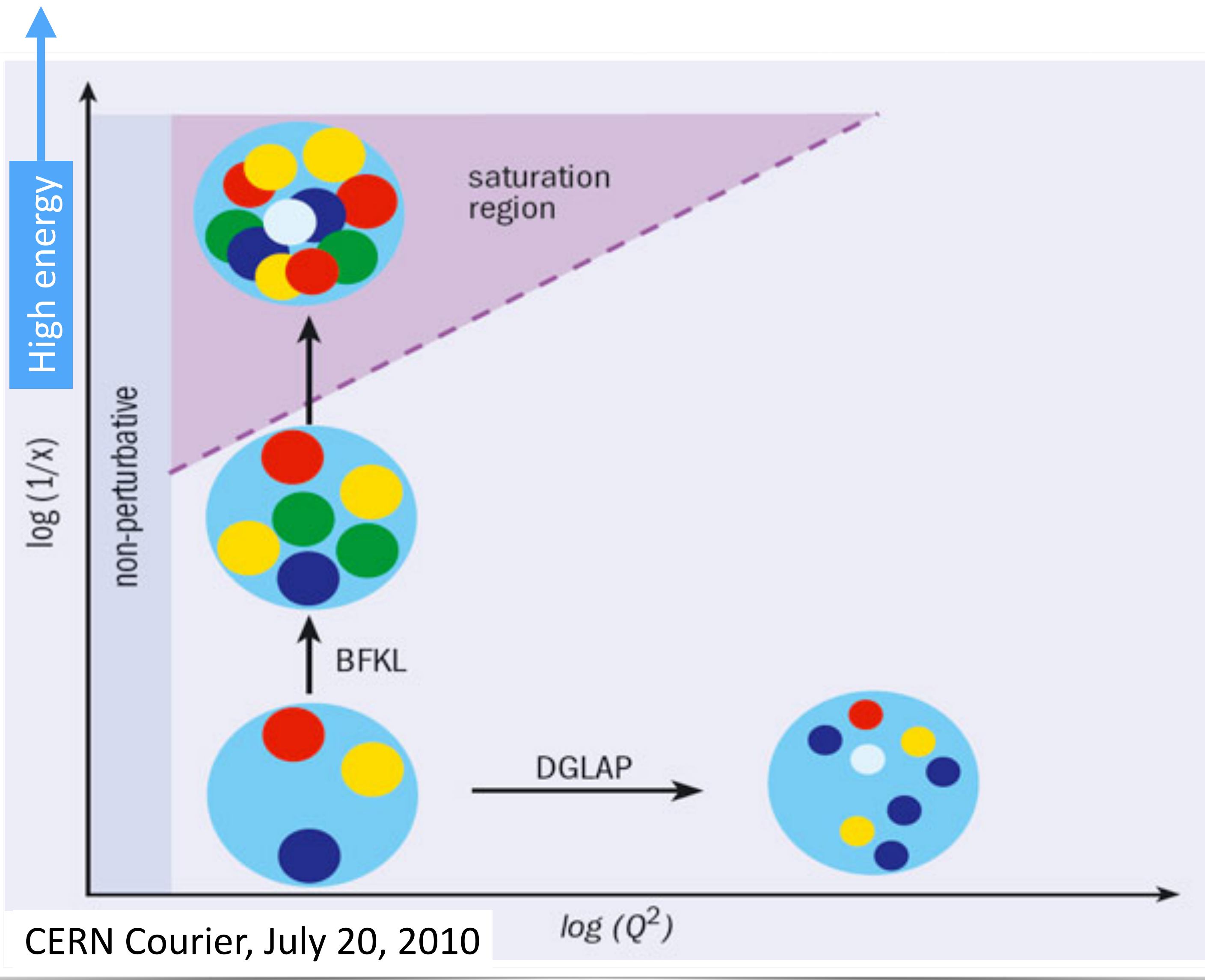
News from J/ψ production in γp collisions

High-energy limit of pQCD



CERN Courier, July 20, 2010

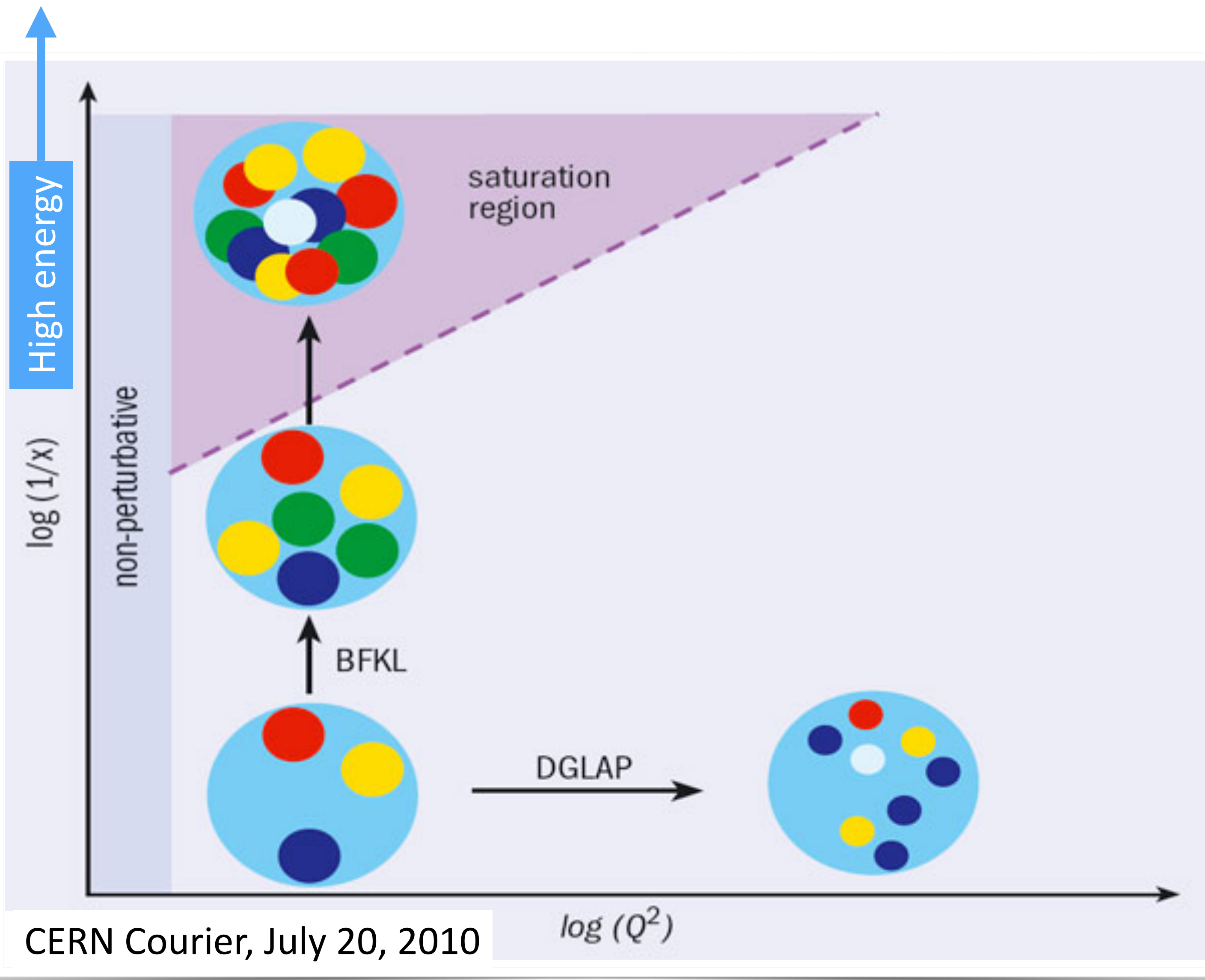
High-energy limit of pQCD



The high-energy limit of pQCD corresponds to the small x limit and in the case of J/ψ photoproduction it is customary to use

$$x = M^2/W^2$$

High-energy limit of pQCD



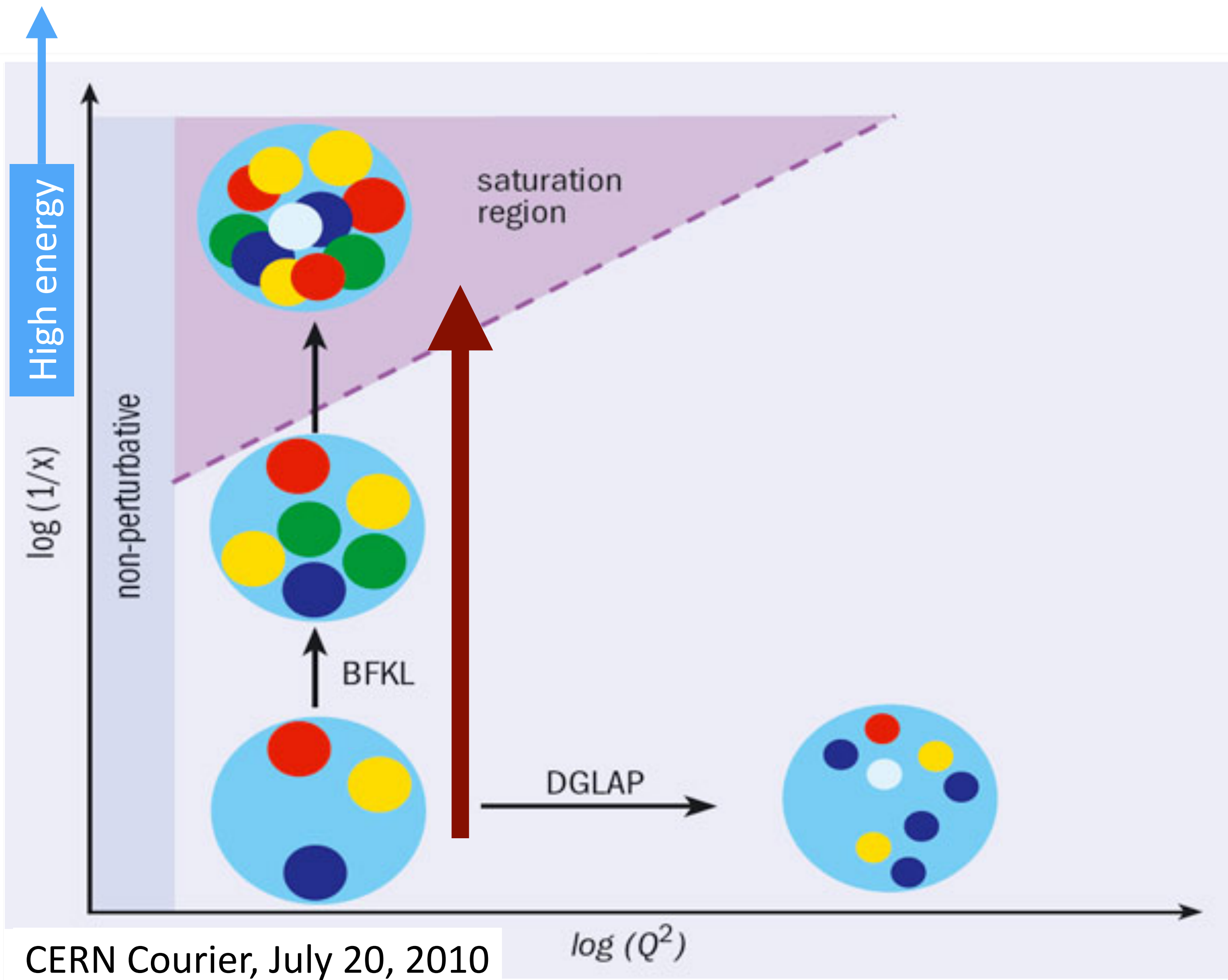
The high-energy limit of pQCD corresponds to the small x limit and in the case of J/ψ photoproduction it is customary to use

$$x = M^2/W^2$$

For photoproduction of J/ψ :

- there is only one hard scale, the mass of the J/ψ , which fixes a point in the $\log(Q^2)$ axis of this diagram,
- the position along the $\log(1/x)$ axis is given by the rapidity of the J/ψ .

High-energy limit of pQCD



The high-energy limit of pQCD corresponds to the small x limit and in the case of J/ψ photoproduction it is customary to use

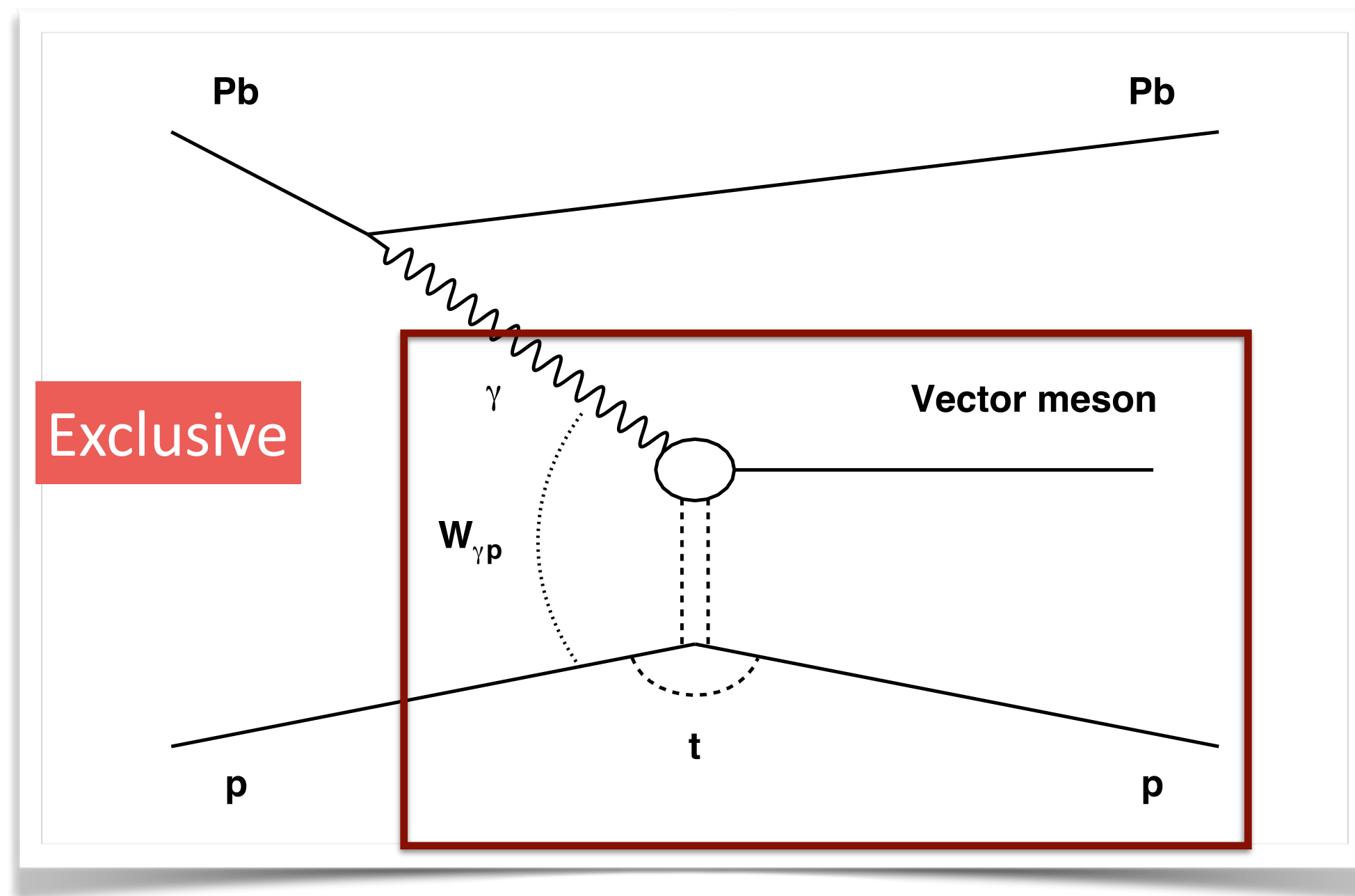
$$x = M^2/W^2$$

For photoproduction of J/ψ :

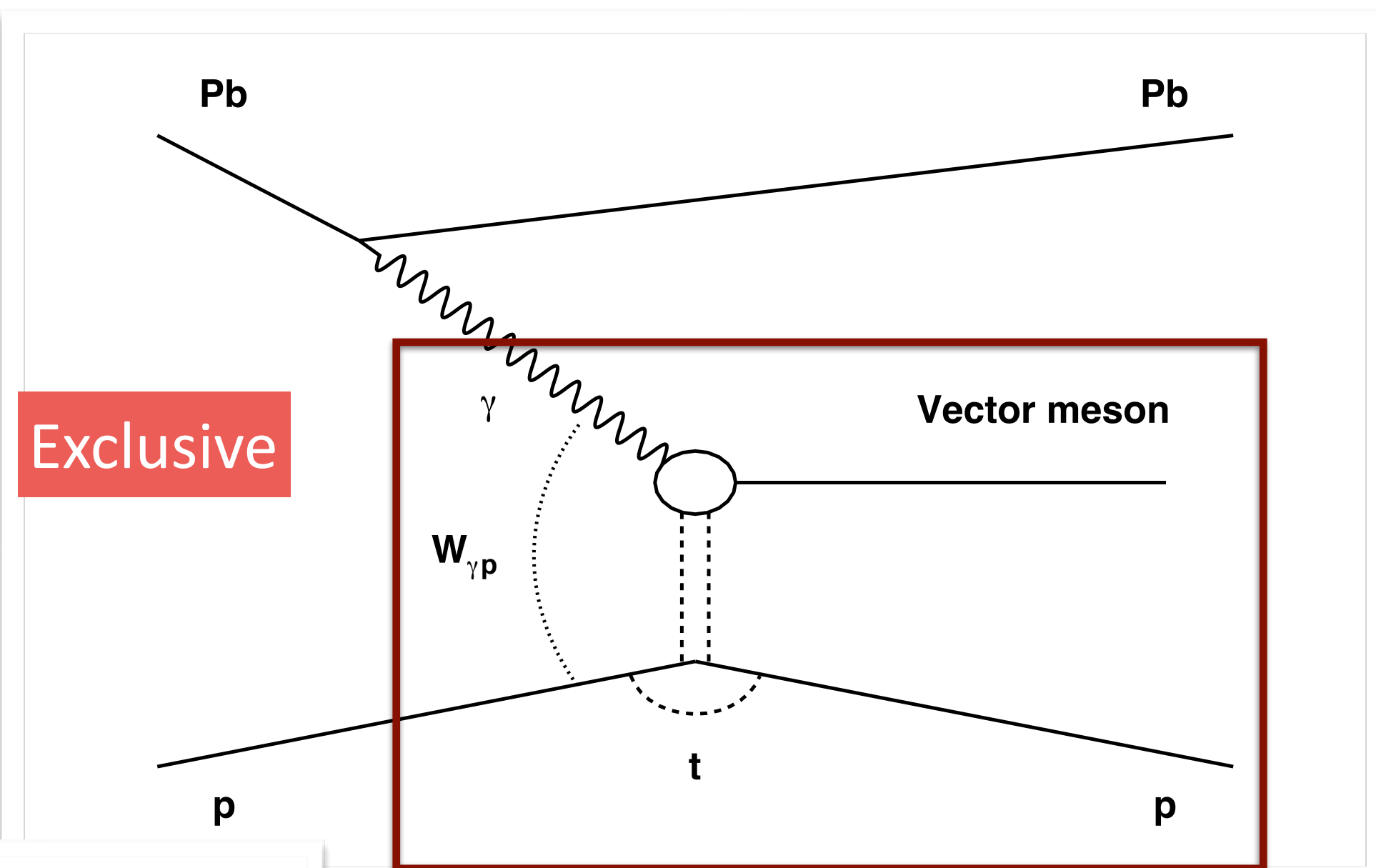
- there is only one hard scale, the mass of the J/ψ , which fixes a point in the $\log(Q^2)$ axis of this diagram,
- the position along the $\log(1/x)$ axis is given by the rapidity of the J/ψ .

The rapidity dependence of J/ψ photoproduction take us upwards in this diagram and may allow us to search for the region labelled **saturation**.

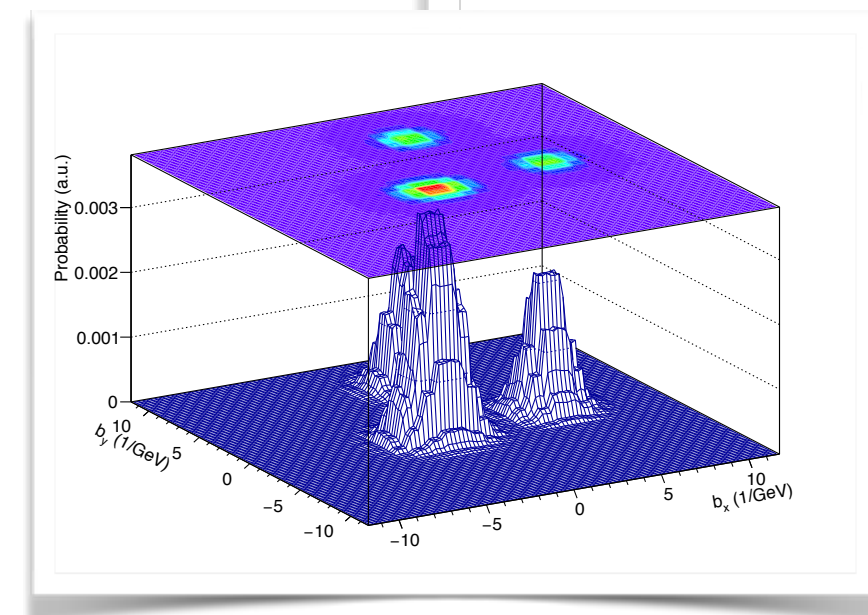
Exclusive and dissociative J/ψ production



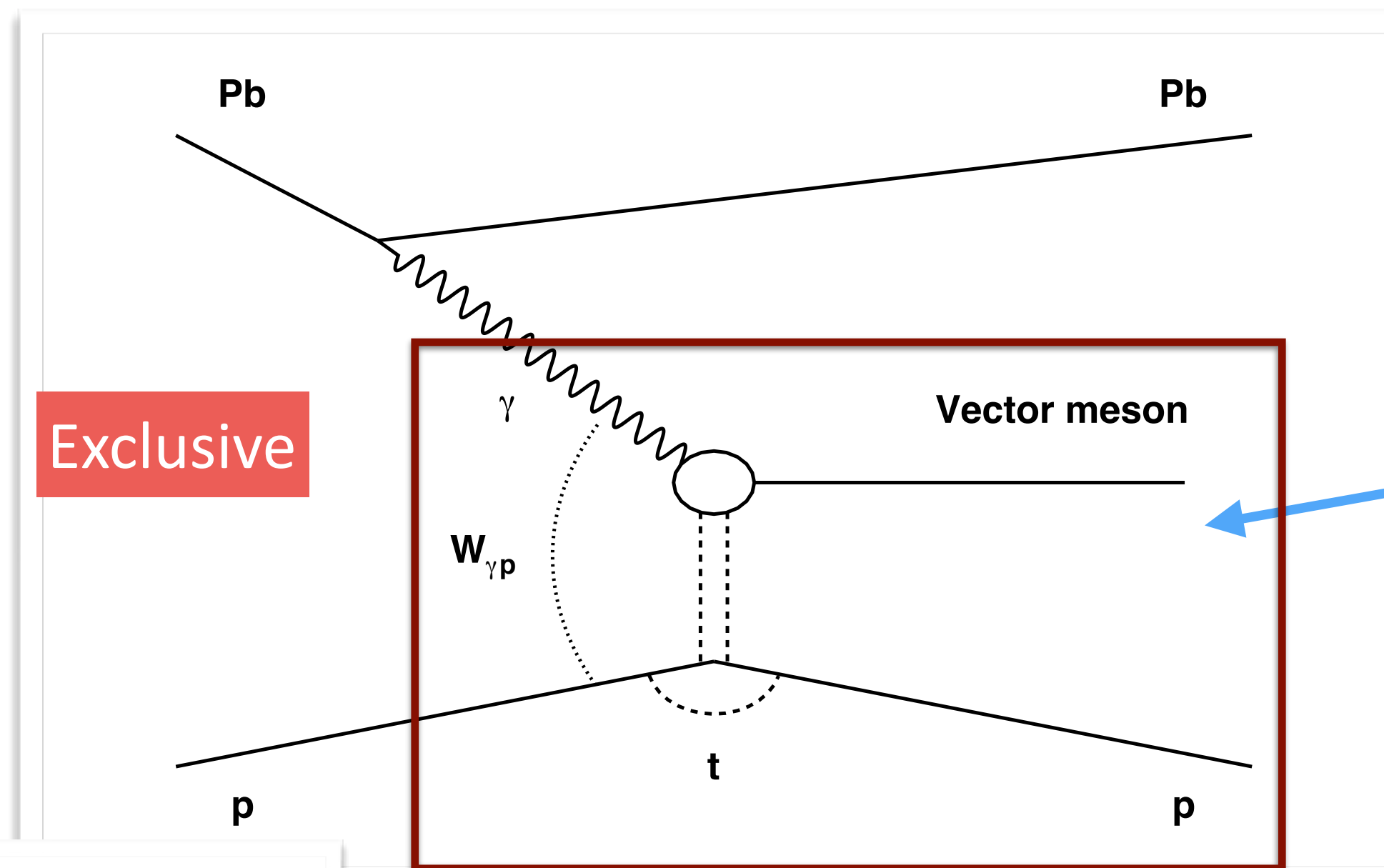
Exclusive and dissociative J/ψ production



Exclusive

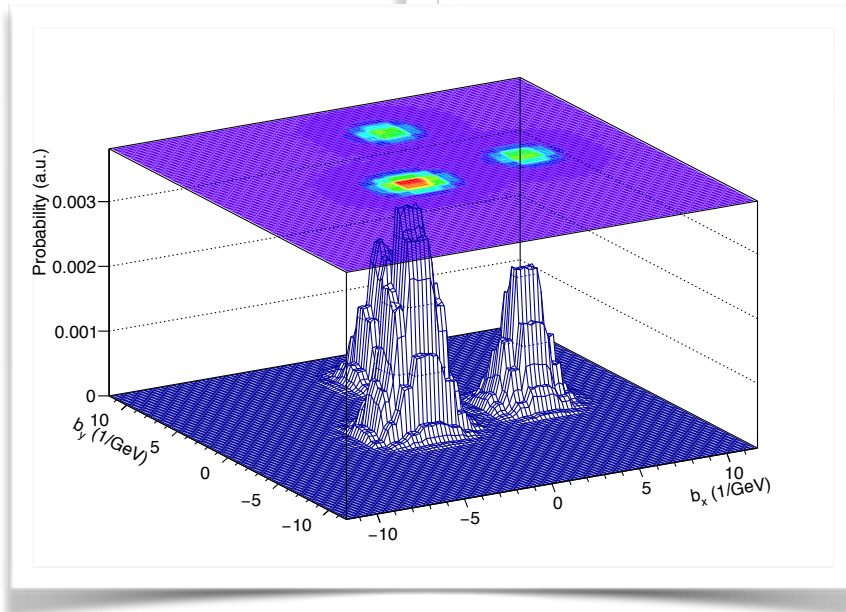


Exclusive and dissociative J/ψ production



$$\frac{d\sigma(\gamma p \rightarrow J/\psi p)}{dt} = \frac{R_g^2}{16\pi} \left| \langle A(x, Q^2, \vec{\Delta}) \rangle \right|^2$$

Average over configurations

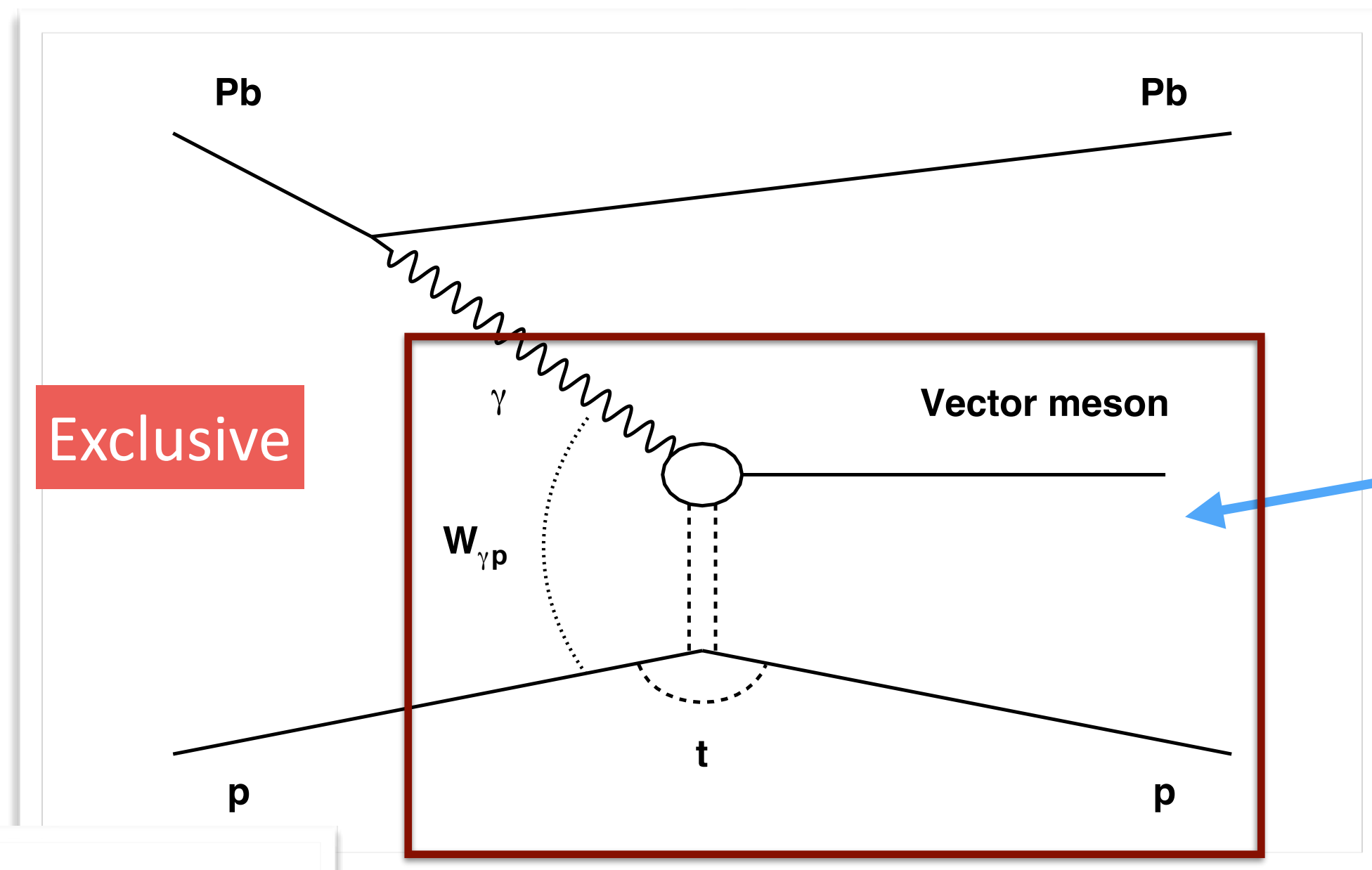


Good, Walker, PR 120 (1960) 1857

Miettinen, Pumplin, PRD18 (1978) 1696

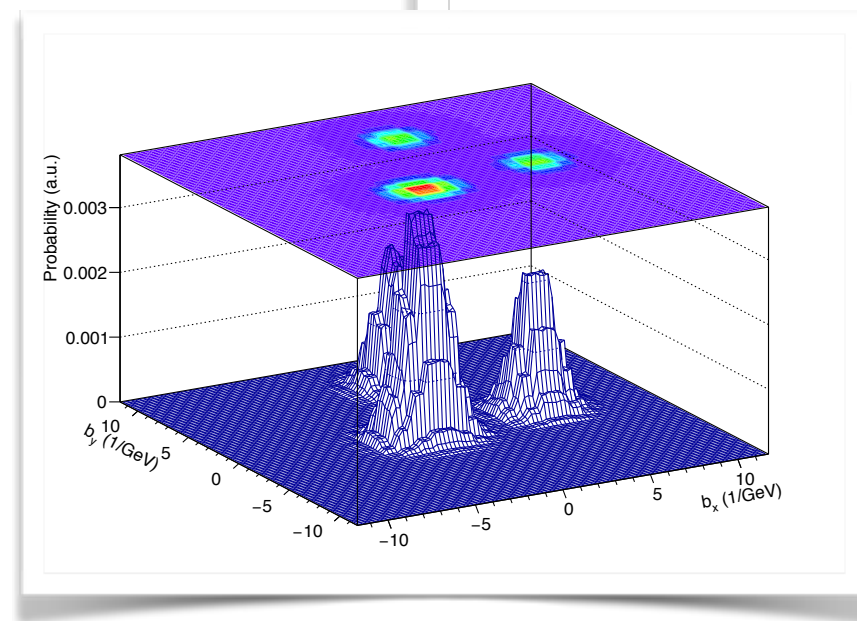
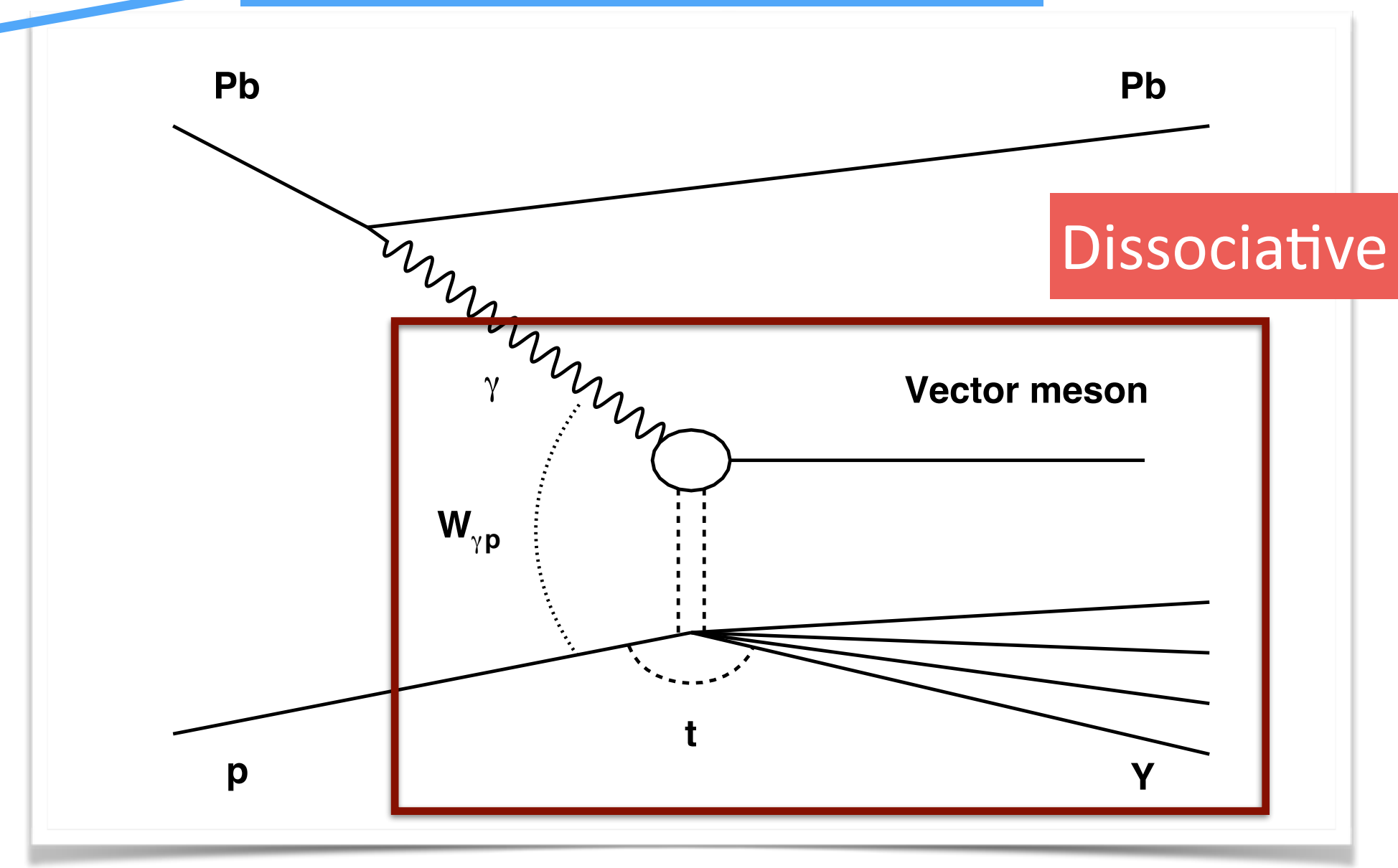
Mantysaari, Schenke, PRL 117 (2016) 052301

Exclusive and dissociative J/ψ production



$$\frac{d\sigma(\gamma p \rightarrow J/\psi p)}{dt} = \frac{R_g^2}{16\pi} \left| \langle A(x, Q^2, \vec{\Delta}) \rangle \right|^2$$

Average over configurations

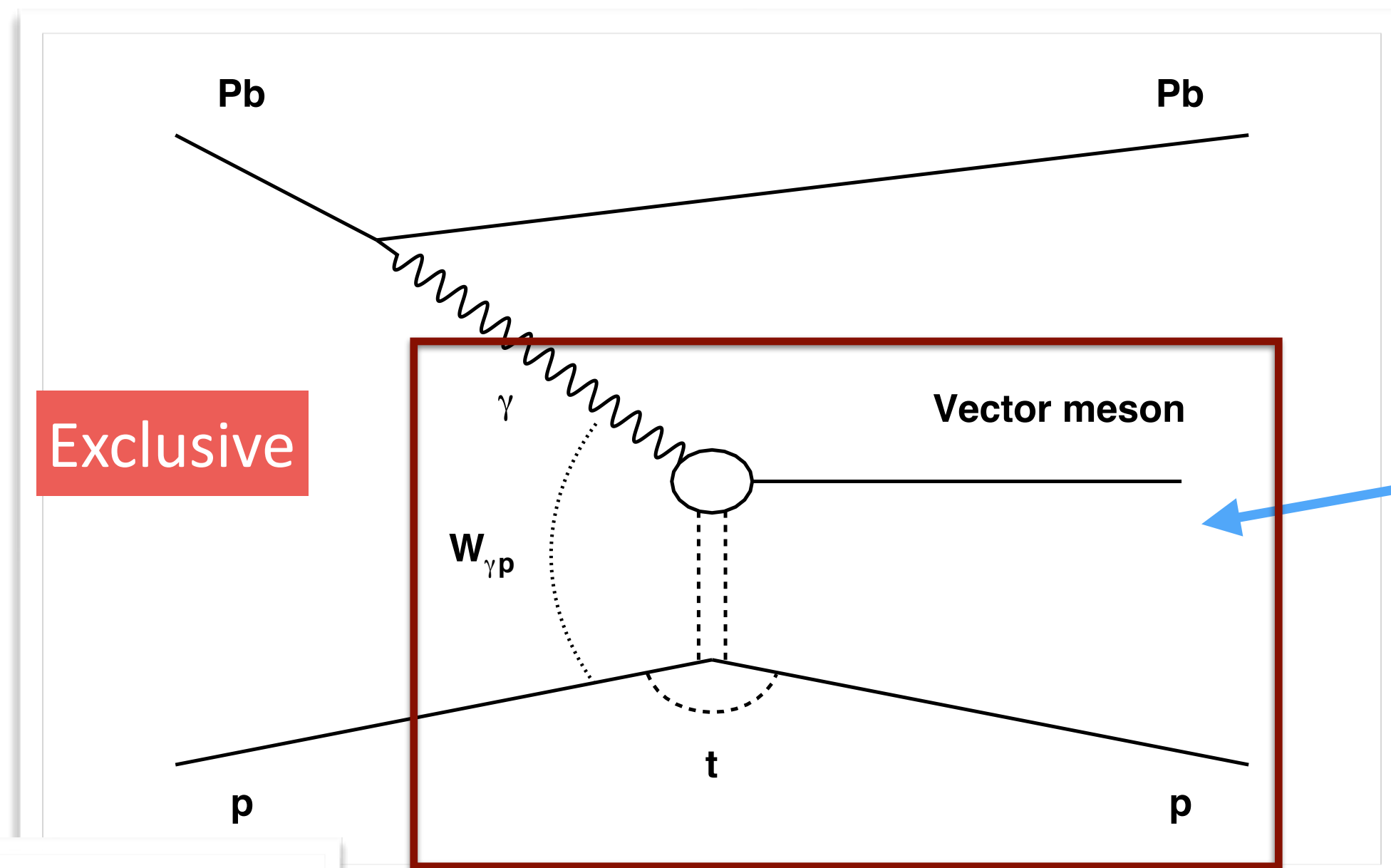


Good, Walker, PR 120 (1960) 1857

Miettinen, Pumplin, PRD18 (1978) 1696

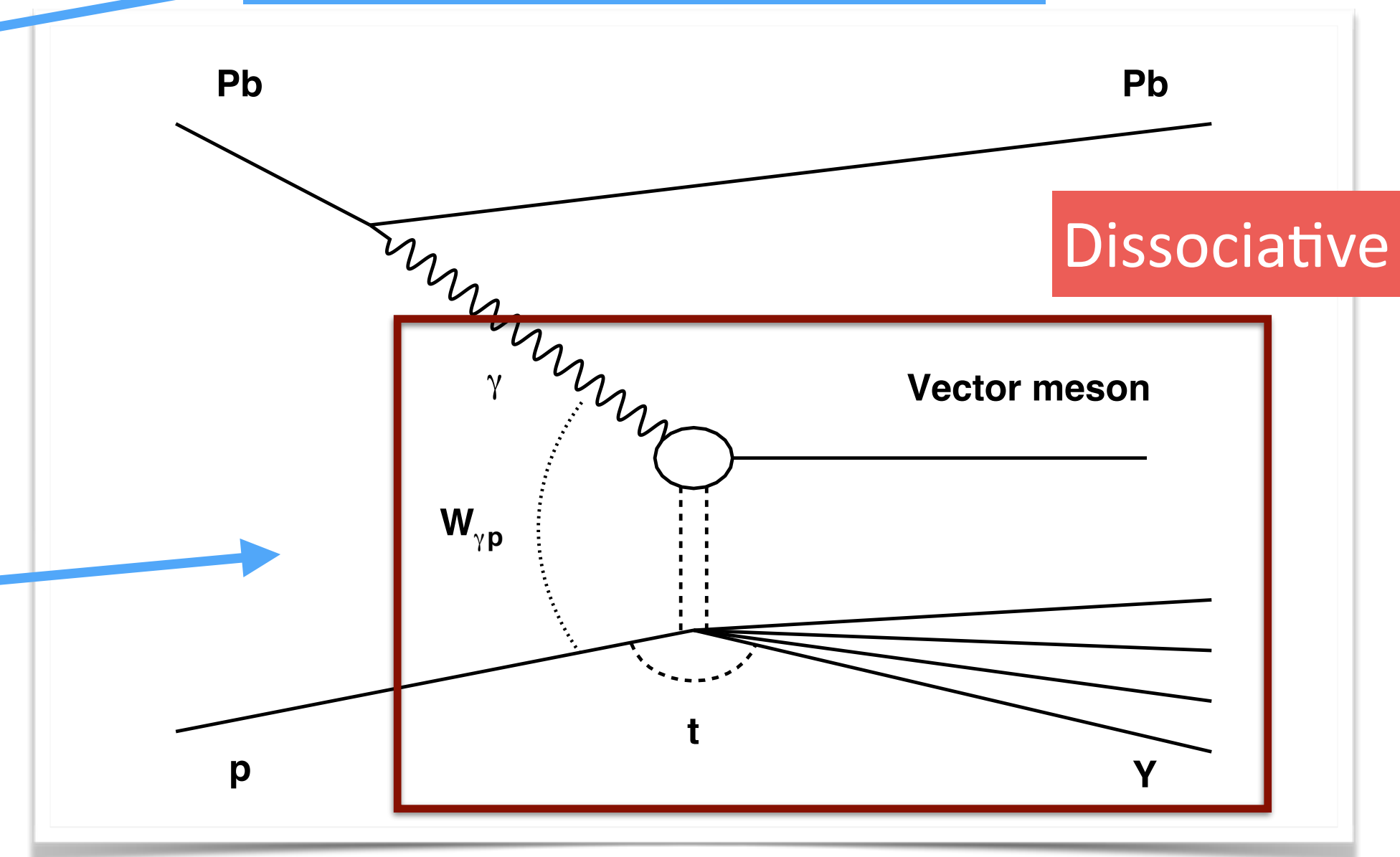
Mantysaari, Schenke, PRL 117 (2016) 052301

Exclusive and dissociative J/ψ production



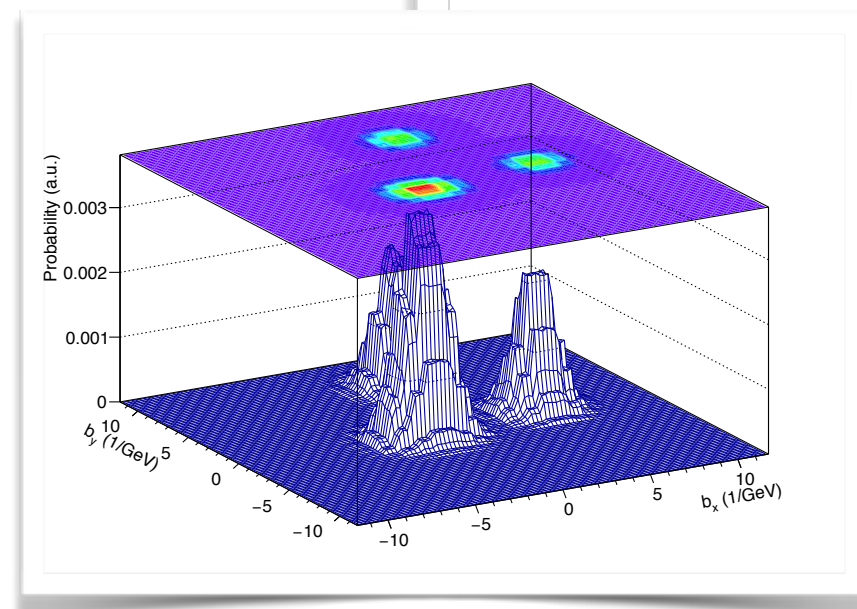
$$\frac{d\sigma(\gamma p \rightarrow J/\psi p)}{dt} = \frac{R_g^2}{16\pi} \left| \langle A(x, Q^2, \vec{\Delta}) \rangle \right|^2$$

Average over configurations



Variance over configurations

$$\frac{d\sigma(\gamma p \rightarrow J/\psi Y)}{dt} = \frac{R_g^2}{16\pi} \left(\langle |A(x, Q^2, \vec{\Delta})|^2 \rangle - \left| \langle A(x, Q^2, \vec{\Delta}) \rangle \right|^2 \right)$$

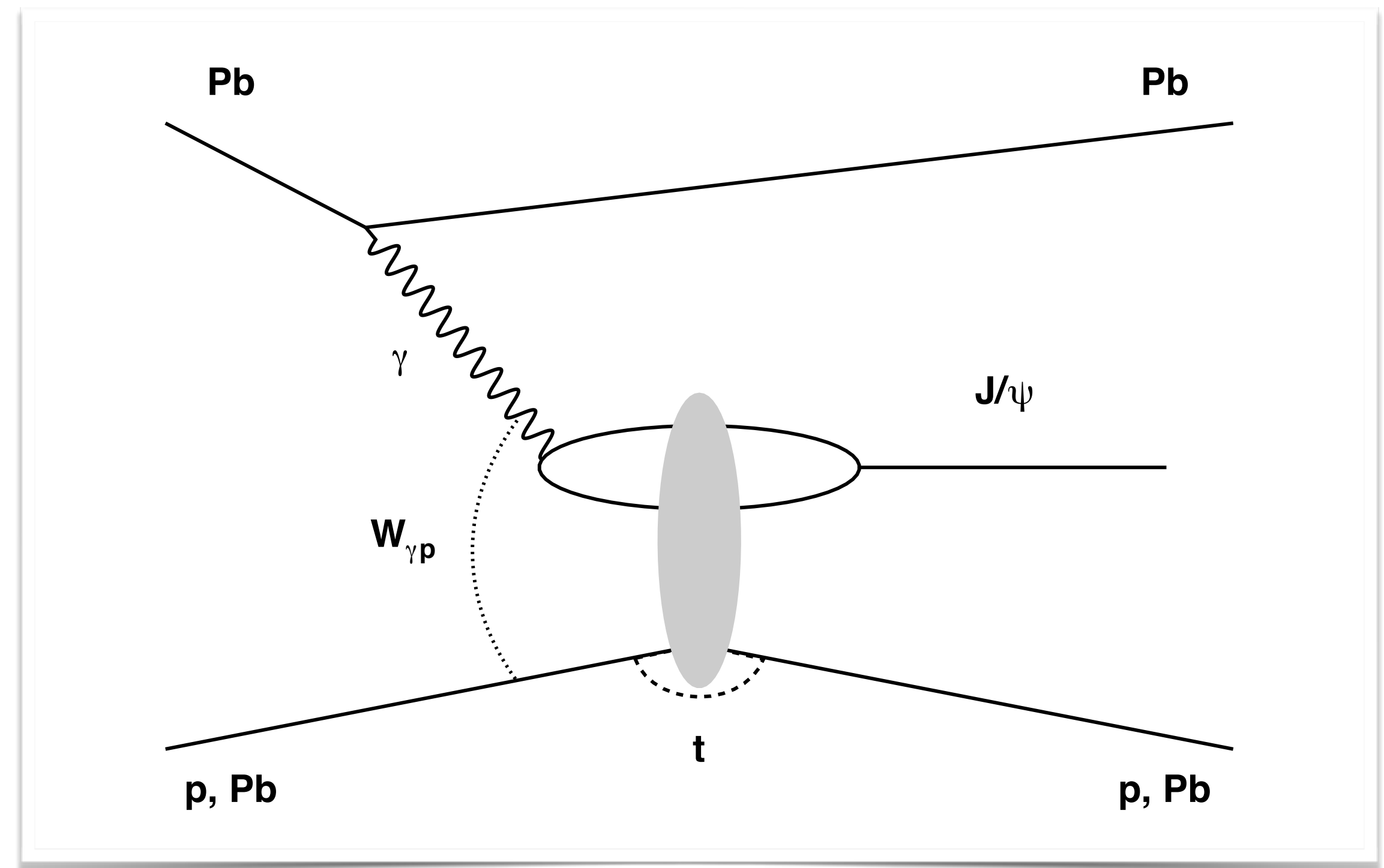


Good, Walker, PR 120 (1960) 1857

Miettinen, Pumplin, PRD18 (1978) 1696

Mantysaari, Schenke, PRL 117 (2016) 052301

The amplitude in the dipole picture

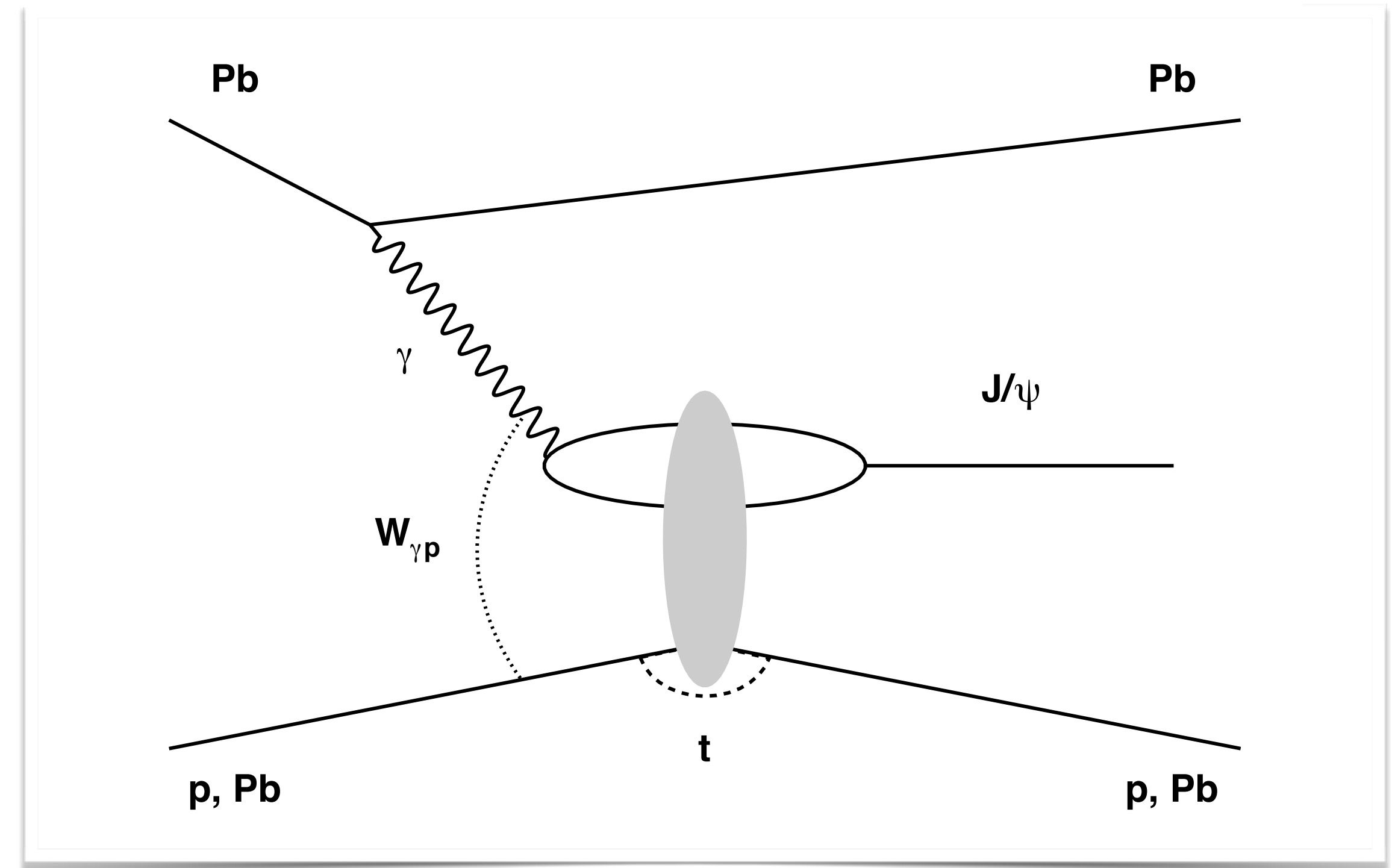


e.g., Kowalski, Motyka, Watt, PRD74 (2006) 074016

The amplitude in the dipole picture

x related to $W_{\gamma p}$ which is related to the rapidity of the vector meson

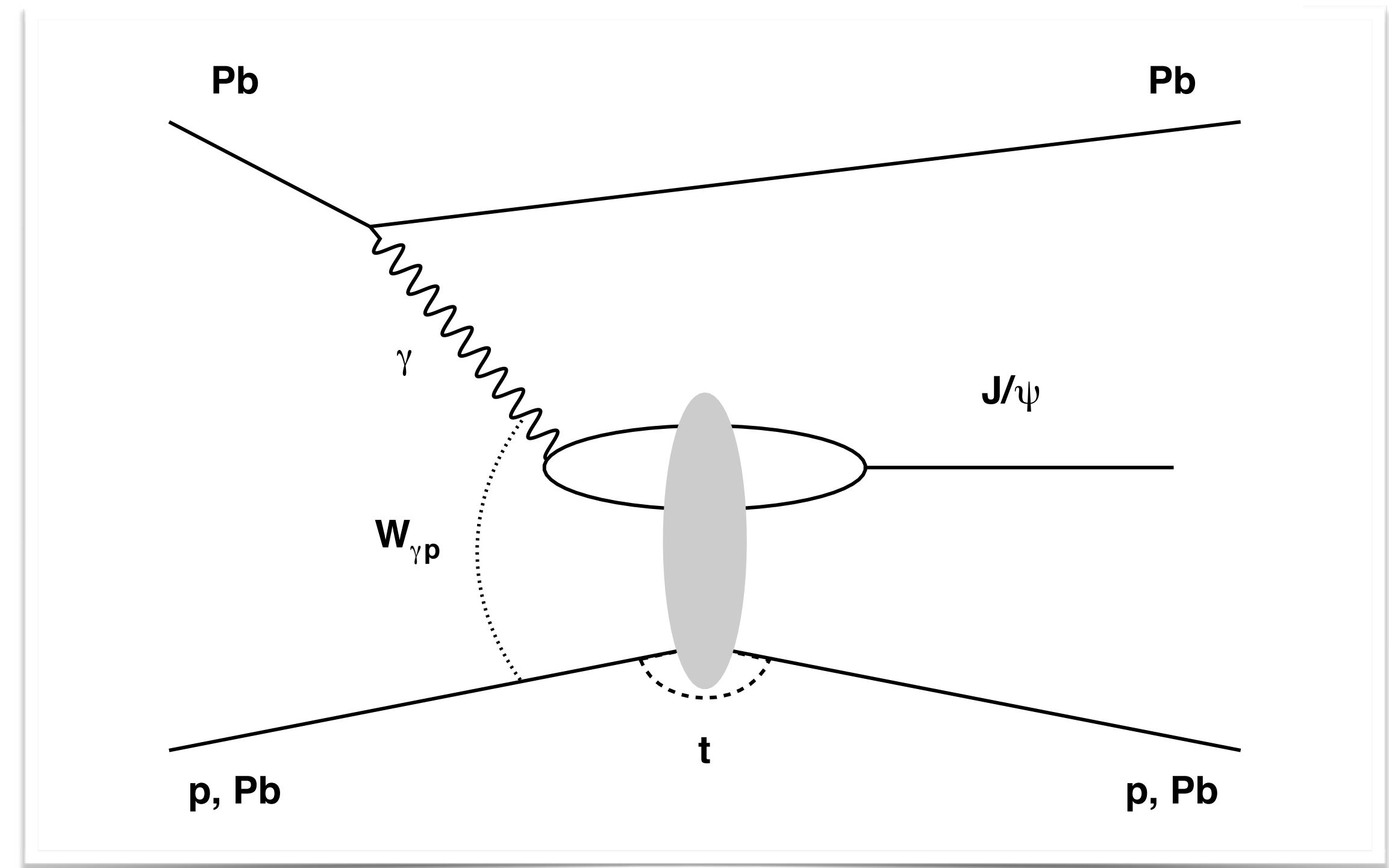
$$A(x, Q^2, \vec{\Delta})_{T,L} = i \int d\vec{r} \int_0^1 \frac{dz}{4\pi} (\Psi^* \Psi_V)_{T,L} \int d\vec{b} e^{-i(\vec{b} - (1-z)\vec{r}) \cdot \vec{\Delta}} \frac{d\sigma_{\text{dip}}}{d\vec{b}}$$



The amplitude in the dipole picture

x related to $W_{\gamma p}$ which is related to the rapidity of the vector meson

$$A(x, Q^2, \vec{\Delta})_{T,L} = i \int d\vec{r} \int_0^1 \frac{dz}{4\pi} (\Psi^* \Psi_V)_{T,L} \int d\vec{b} e^{-i(\vec{b} - (1-z)\vec{r}) \cdot \vec{\Delta}} \frac{d\sigma_{\text{dip}}}{d\vec{b}}$$



e.g., Kowalski, Motyka, Watt, PRD74 (2006) 074016

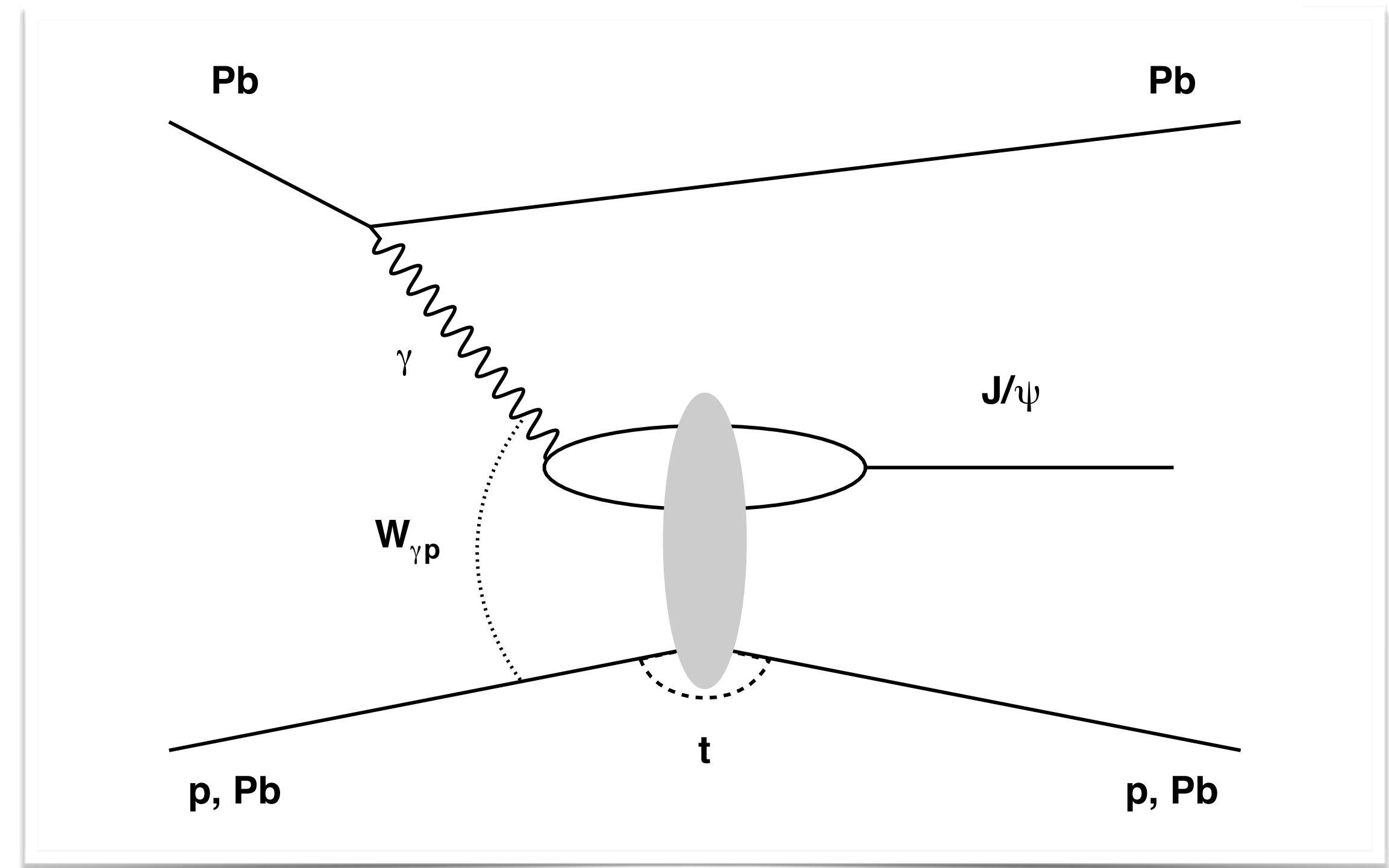
The amplitude in the dipole picture

x related to $W_{\gamma p}$ which is related to the rapidity of the vector meson

$\Delta^2 = -t$

Quark energy fraction

$$A(x, Q^2, \vec{\Delta})_{T,L} = i \int d\vec{r} \int_0^1 \frac{dz}{4\pi} (\Psi^* \Psi_V)_{T,L} \int d\vec{b} e^{-i(\vec{b} - (1-z)\vec{r}) \cdot \vec{\Delta}} \frac{d\sigma_{\text{dip}}}{d\vec{b}}$$



The amplitude in the dipole picture

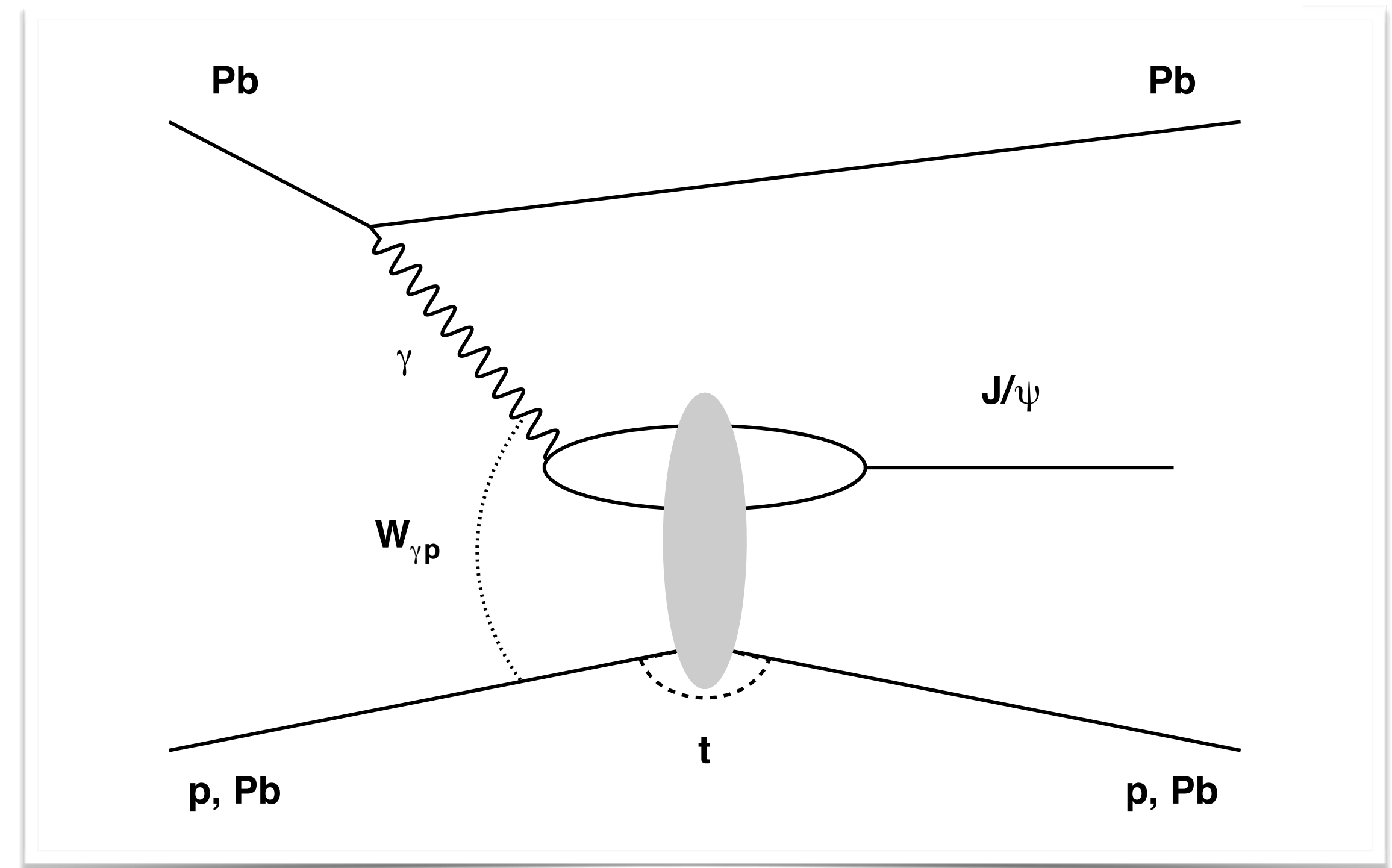
x related to $W_{\gamma p}$ which is related to the rapidity of the vector meson

$$A(x, Q^2, \vec{\Delta})_{T,L} = i \int d\vec{r} \int_0^1 \frac{dz}{4\pi} (\Psi^* \Psi_V)_{T,L} \int d\vec{b} e^{-i(\vec{b} - (1-z)\vec{r}) \cdot \vec{\Delta}} \frac{d\sigma_{\text{dip}}}{d\vec{b}}$$

$\Delta^2 = -t$

Dipole size

Quark energy fraction



The amplitude in the dipole picture

x related to $W_{\gamma p}$ which is related to the rapidity of the vector meson

$$A(x, Q^2, \vec{\Delta})_{T,L} = i \int d\vec{r} \int_0^1 \frac{dz}{4\pi} (\Psi^* \Psi_V)_{T,L} \int d\vec{b} e^{-i(\vec{b} - (1-z)\vec{r}) \cdot \vec{\Delta}} \frac{d\sigma_{\text{dip}}}{d\vec{b}}$$

$\Delta^2 = -t$

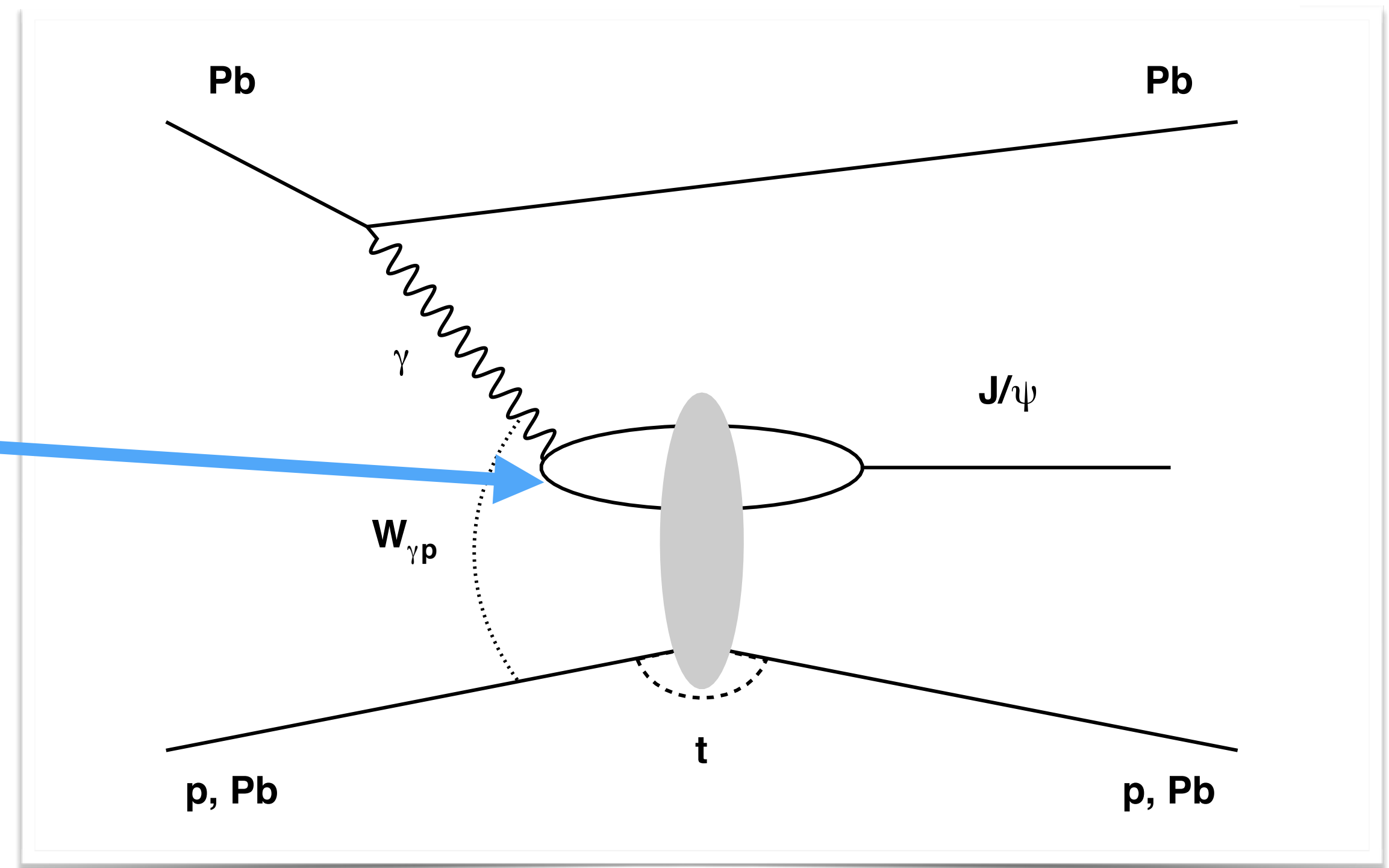
Dipole size

Quark energy fraction

Transverse, Longitudinal photons

Photon-dipole wave function

Photon virtuality



e.g., Kowalski, Motyka, Watt, PRD74 (2006) 074016

The amplitude in the dipole picture

x related to $W_{\gamma p}$ which is related to the rapidity of the vector meson

$$A(x, Q^2, \vec{\Delta})_{T,L} = i \int d\vec{r} \int_0^1 \frac{dz}{4\pi} (\Psi^* \Psi_V)_{T,L} \int d\vec{b} e^{-i(\vec{b} - (1-z)\vec{r}) \cdot \vec{\Delta}} \frac{d\sigma_{\text{dip}}}{d\vec{b}}$$

$\Delta^2 = -t$

Dipole size

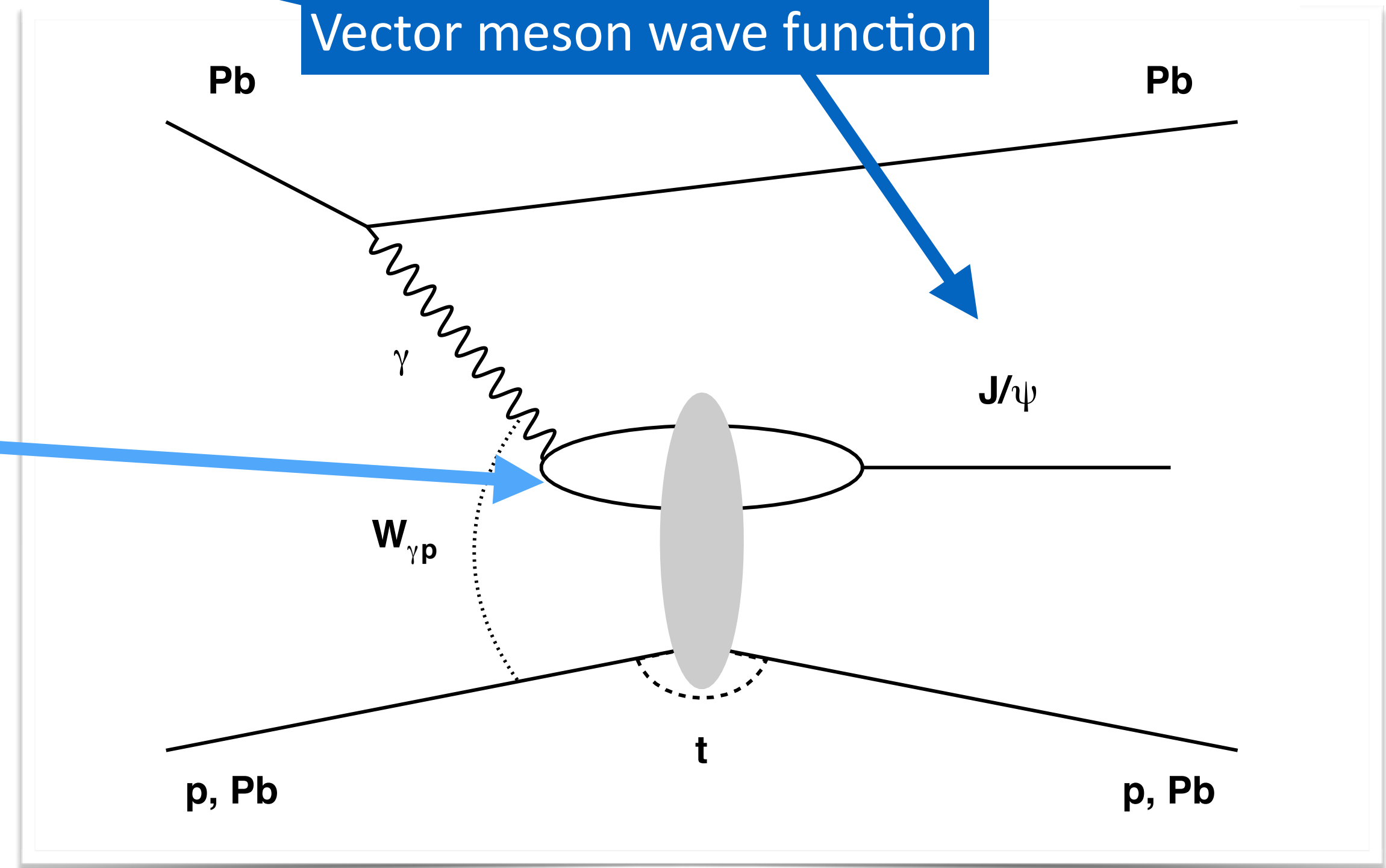
Quark energy fraction

Transverse, Longitudinal photons

Photon virtuality

Photon-dipole wave function

Vector meson wave function



The amplitude in the dipole picture

x related to $W_{\gamma p}$ which is related to the rapidity of the vector meson

$$A(x, Q^2, \vec{\Delta})_{T,L} = i \int d\vec{r} \int_0^1 \frac{dz}{4\pi} (\Psi^* \Psi_V)_{T,L} \int d\vec{b} e^{-i(\vec{b} - (1-z)\vec{r}) \cdot \vec{\Delta}} \frac{d\sigma_{\text{dip}}}{d\vec{b}}$$

$\Delta^2 = -t$

Dipole size

Quark energy fraction

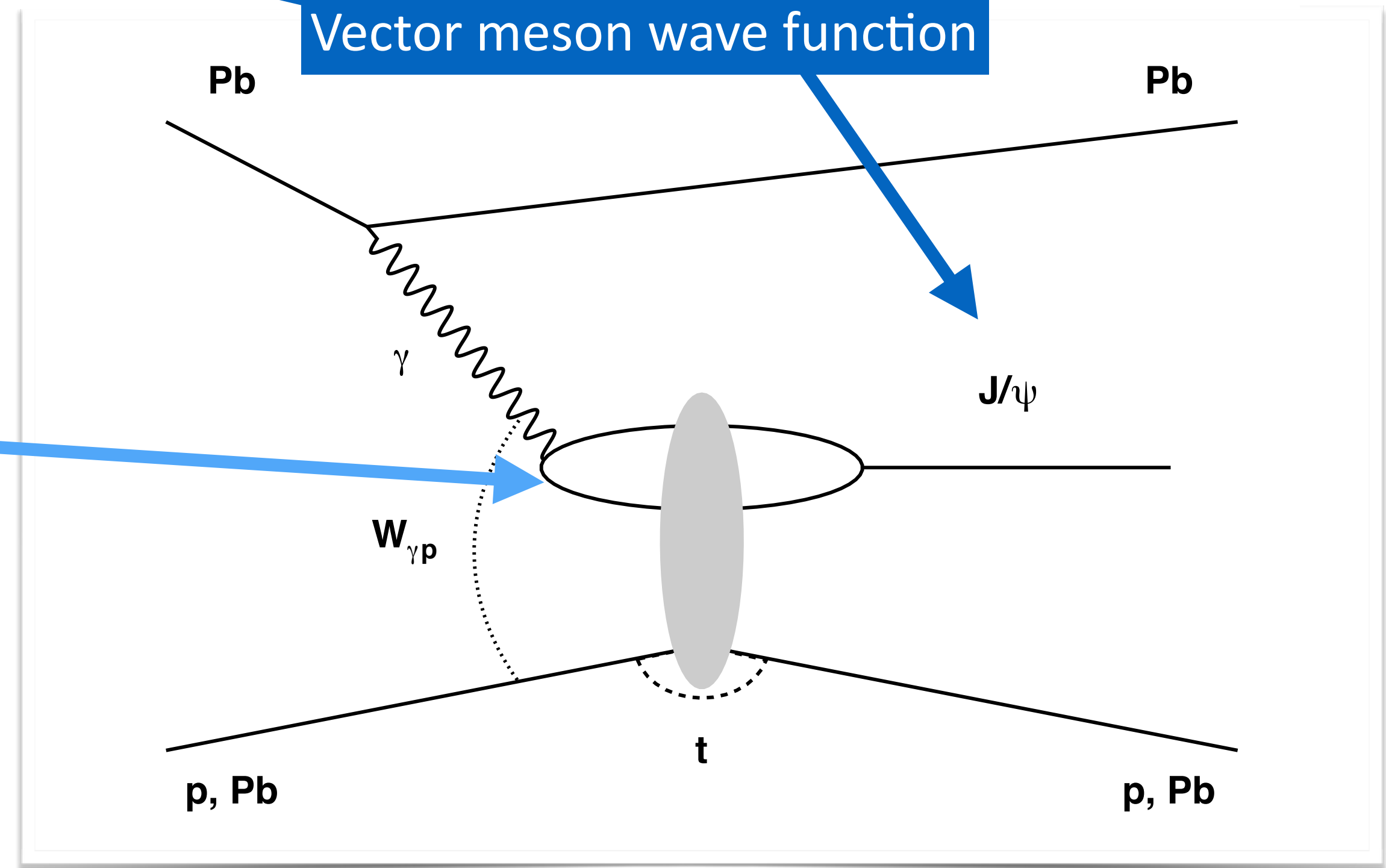
Impact parameter

Transverse, Longitudinal photons

Photon virtuality

Photon-dipole wave function

Vector meson wave function

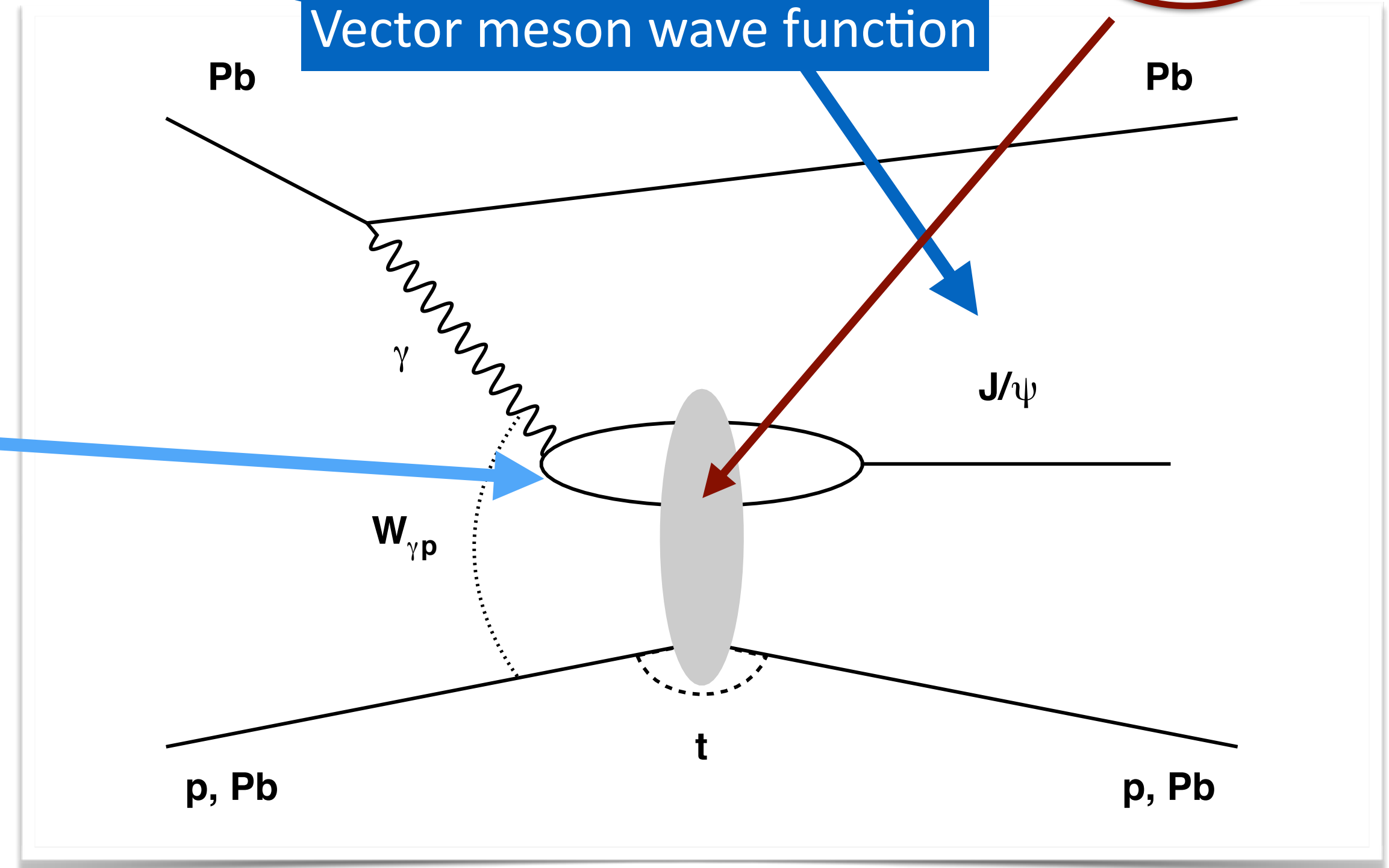
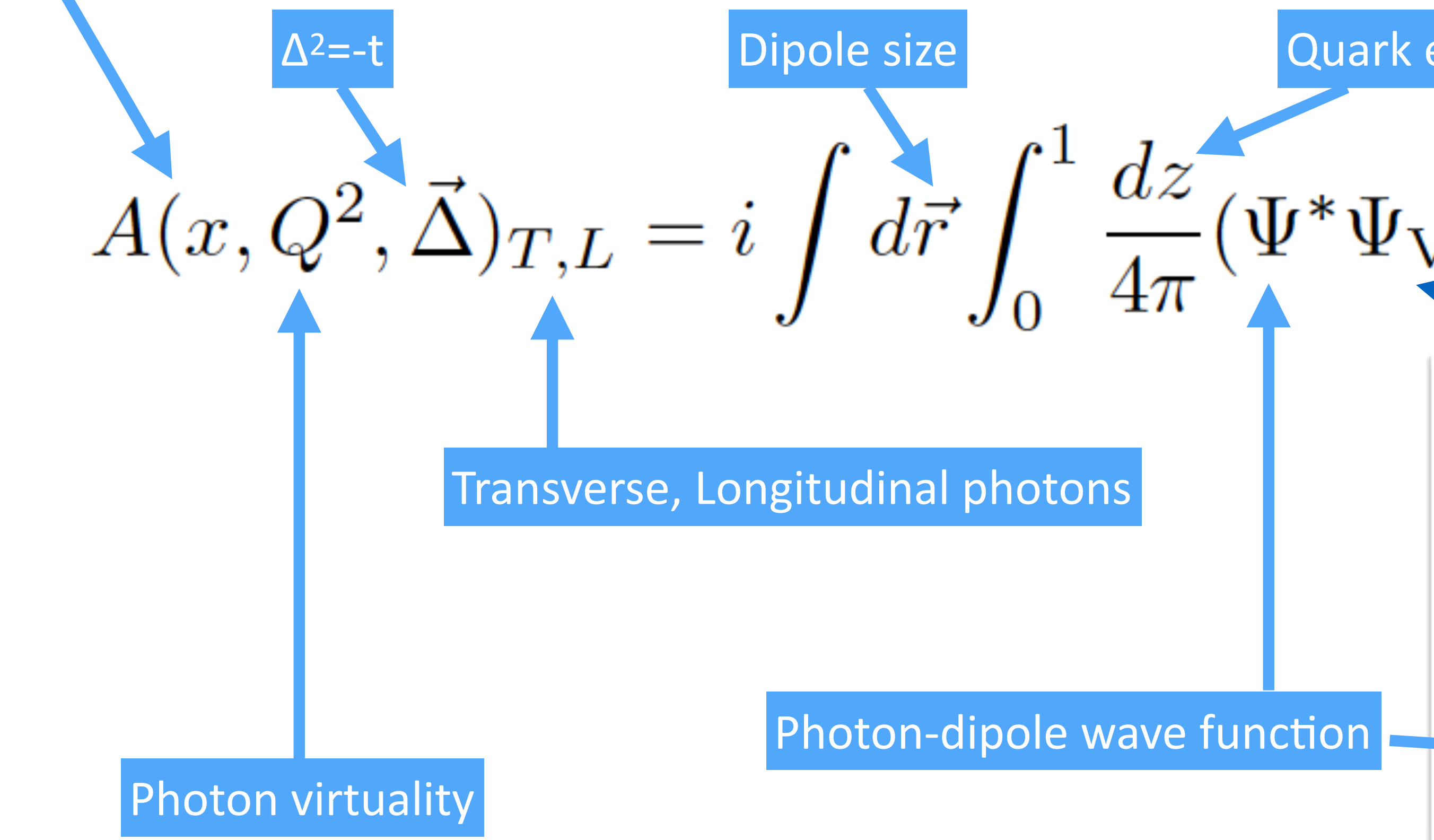


The amplitude in the dipole picture

x related to $W_{\gamma p}$ which is related to the rapidity of the vector meson

Dipole-Target cross section
pQCD physics gets here!

$$A(x, Q^2, \vec{\Delta})_{T,L} = i \int d\vec{r} \int_0^1 \frac{dz}{4\pi} (\Psi^* \Psi_V)_{T,L} \int d\vec{b} e^{-i(\vec{b} - (1-z)\vec{r}) \cdot \vec{\Delta}} \frac{d\sigma_{\text{dip}}}{d\vec{b}}$$



e.g., Kowalski, Motyka, Watt, PRD74 (2006) 074016

The dipole-target cross section

Dipole target amplitude

$$\frac{d\sigma_{\text{dip}}}{d\vec{b}} = 2N(x, \vec{r}, \vec{b})$$

The dipole-target cross section

Dipole target amplitude

$$\frac{d\sigma_{\text{dip}}}{d\vec{b}} = 2N(x, \vec{r}, \vec{b})$$

Factorised assumption

$$N(x, r, b) = \sigma_0 N(x, r) T(\vec{b})$$

The dipole-target cross section

Dipole target amplitude

$$\frac{d\sigma_{\text{dip}}}{d\vec{b}} = 2N(x, \vec{r}, \vec{b})$$

Factorised assumption

$$N(x, r, b) = \sigma_0 N(x, r) T(\vec{b})$$

Golec-Biernat Wuesthoff model

$$N^{\text{GBW}}(x, r) = \left(1 - e^{-r^2 Q_s^2(x)/4}\right)$$

$$Q_s^2(x) = Q_0^2(x_0/x)^\lambda$$

The dipole-target cross section

Dipole target amplitude

$$\frac{d\sigma_{\text{dip}}}{d\vec{b}} = 2N(x, \vec{r}, \vec{b})$$

Factorised assumption

$$N(x, r, b) = \sigma_0 N(x, r) T(\vec{b})$$

Golec-Biernat Wuesthoff model

$$N^{\text{GBW}}(x, r) = \left(1 - e^{-r^2 Q_s^2(x)/4}\right)$$

$$Q_s^2(x) = Q_0^2(x_0/x)^\lambda$$

Proton is a sum of hot spots

$$T(\vec{b}) = \frac{1}{N_{hs}} \sum_{i=1}^{N_{hs}} T_{hs}(\vec{b} - \vec{b}_i)$$

The dipole-target cross section

Dipole target amplitude

$$\frac{d\sigma_{\text{dip}}}{d\vec{b}} = 2N(x, \vec{r}, \vec{b})$$

Factorised assumption

$$N(x, r, b) = \sigma_0 N(x, r) T(\vec{b})$$

Golec-Biernat Wuesthoff model

$$N^{\text{GBW}}(x, r) = \left(1 - e^{-r^2 Q_s^2(x)/4}\right)$$

$$Q_s^2(x) = Q_0^2(x_0/x)^\lambda$$

Proton is a sum of hot spots

$$T(\vec{b}) = \frac{1}{N_{hs}} \sum_{i=1}^{N_{hs}} T_{hs}(\vec{b} - \vec{b}_i)$$

Gaussian hot spots

$$T_{hs}(\vec{b} - \vec{b}_i) = \frac{1}{2\pi B_{hs}} e^{-\frac{(\vec{b} - \vec{b}_i)^2}{2B_{hs}}}$$

The dipole-target cross section

Dipole target amplitude

$$\frac{d\sigma_{\text{dip}}}{d\vec{b}} = 2N(x, \vec{r}, \vec{b})$$

Factorised assumption

$$N(x, r, b) = \sigma_0 N(x, r) T(\vec{b})$$

Golec-Biernat Wuesthoff model

$$N^{\text{GBW}}(x, r) = \left(1 - e^{-r^2 Q_s^2(x)/4}\right)$$

Proton is a sum of hot spots

$$T(\vec{b}) = \frac{1}{N_{hs}} \sum_{i=1}^{N_{hs}} T_{hs}(\vec{b} - \vec{b}_i)$$

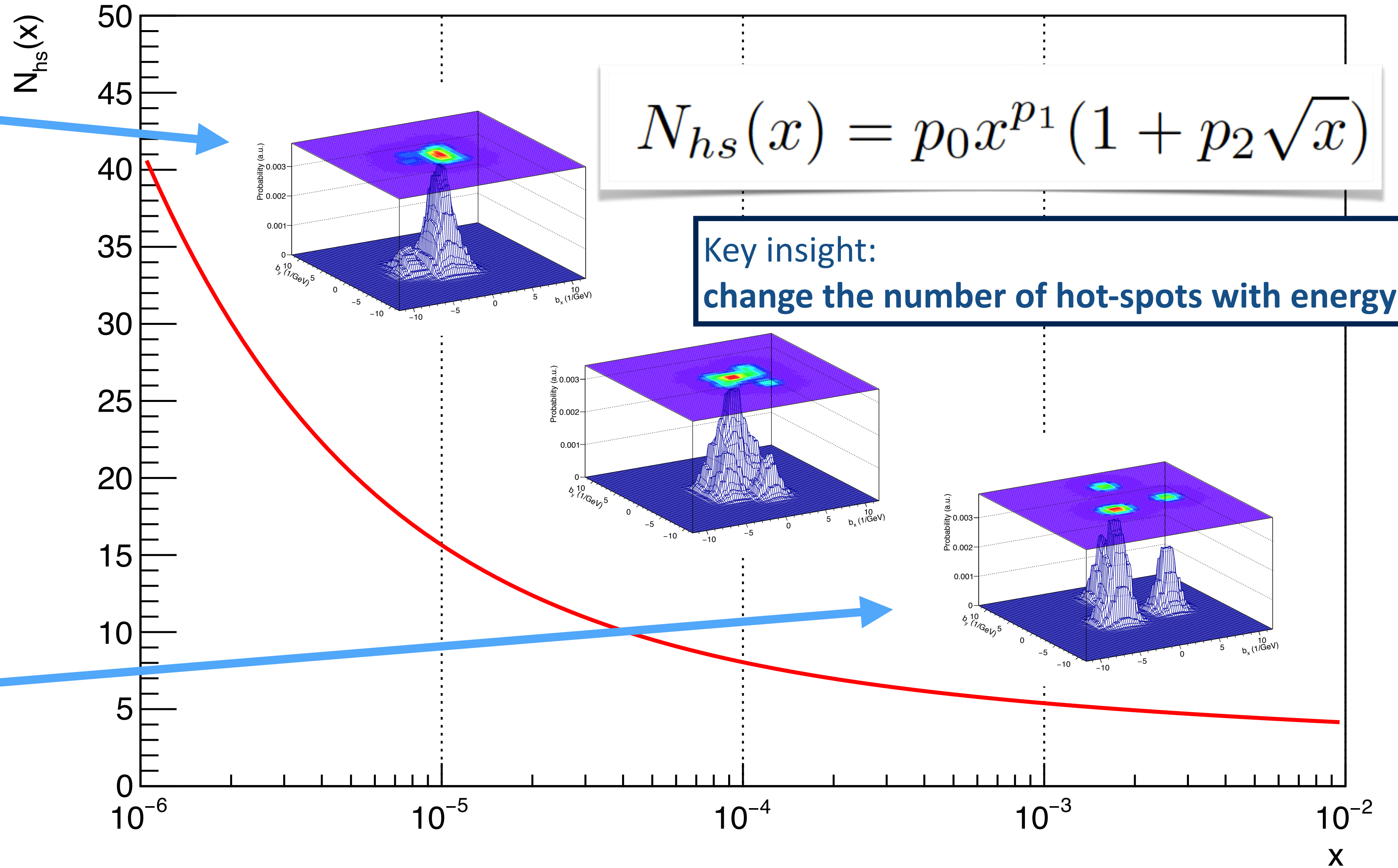
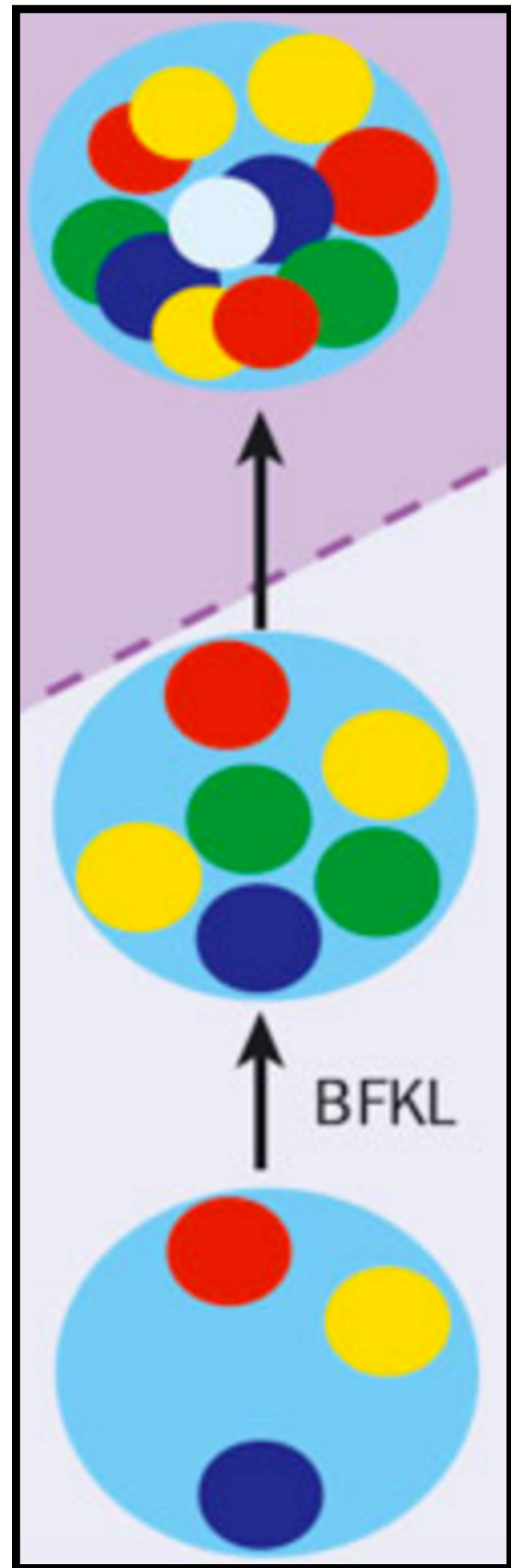
Gaussian hot spots

$$T_{hs}(\vec{b} - \vec{b}_i) = \frac{1}{2\pi B_{hs}} e^{-\frac{(\vec{b} - \vec{b}_i)^2}{2B_{hs}}}$$

Number of hot spots

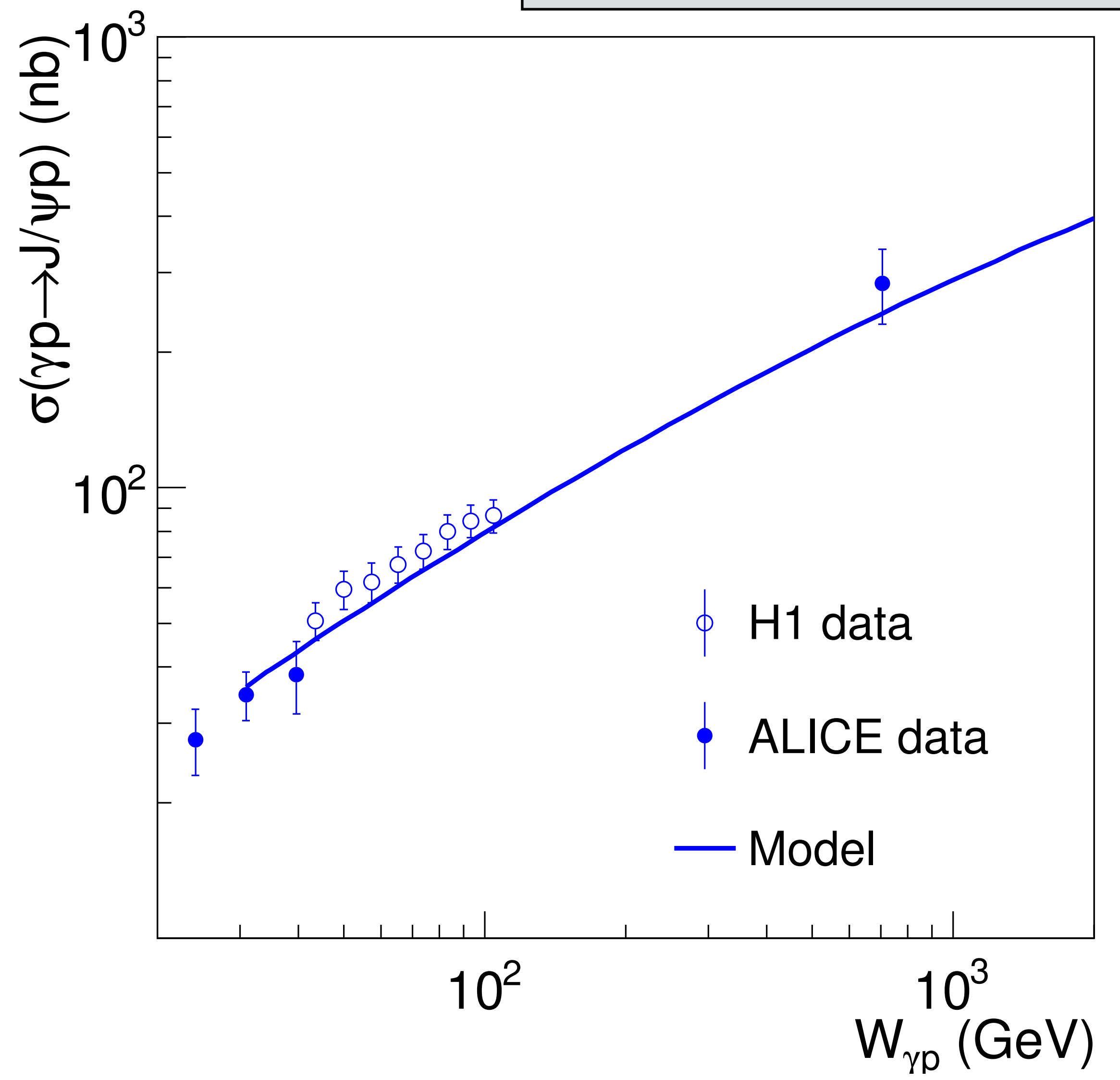
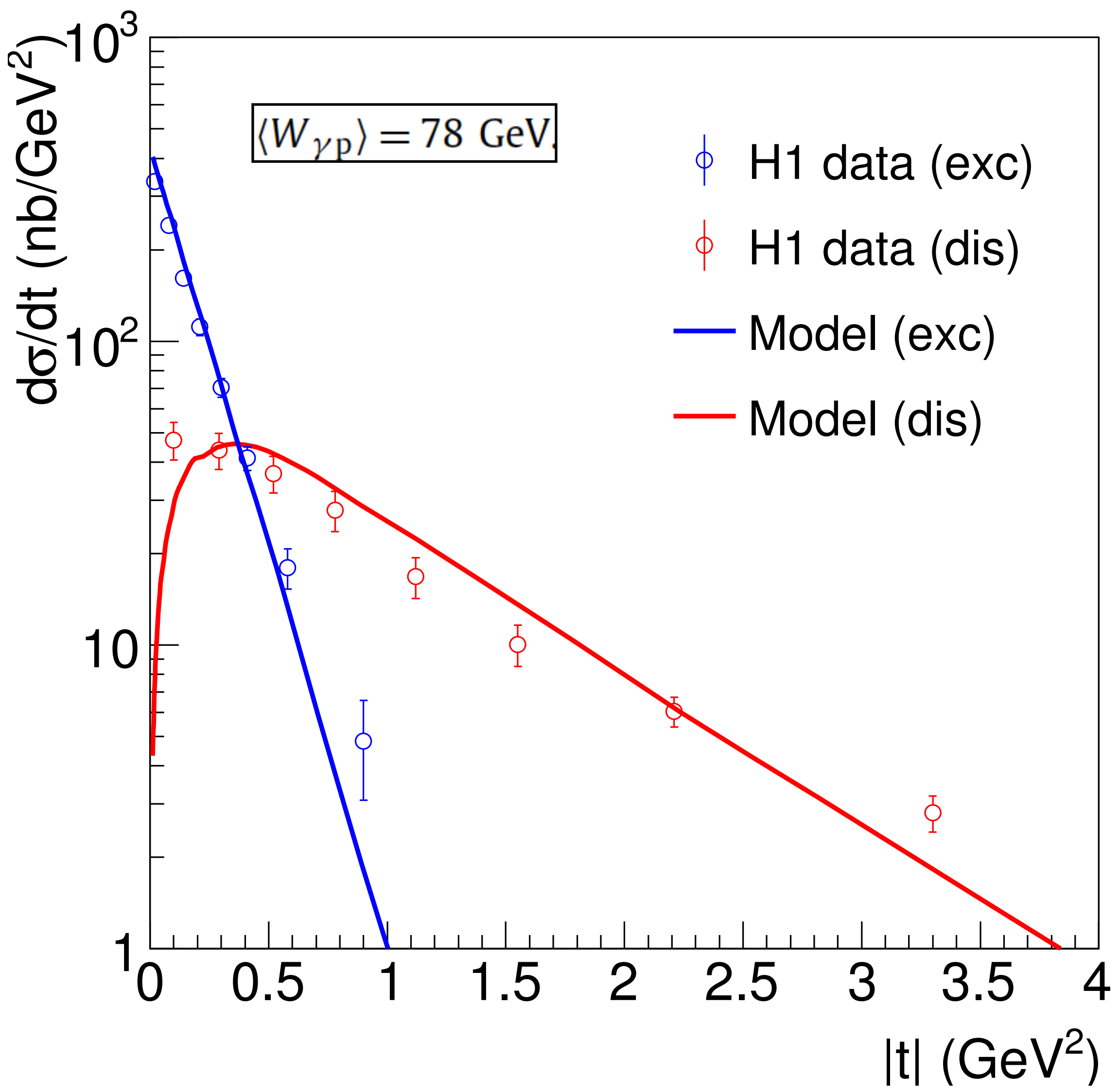
Key insight:
change the number of hot-spots with energy!

Number of hot spots



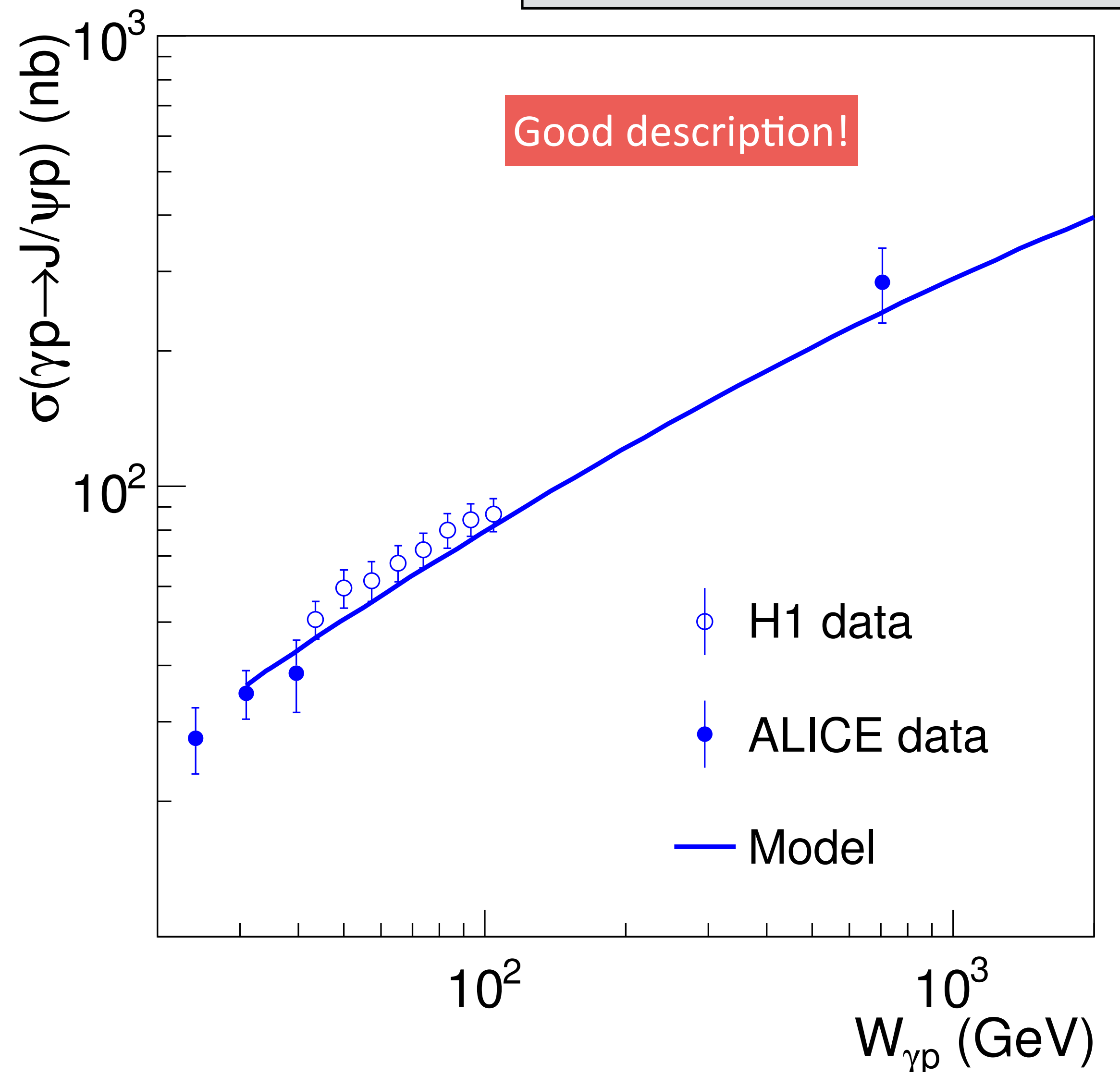
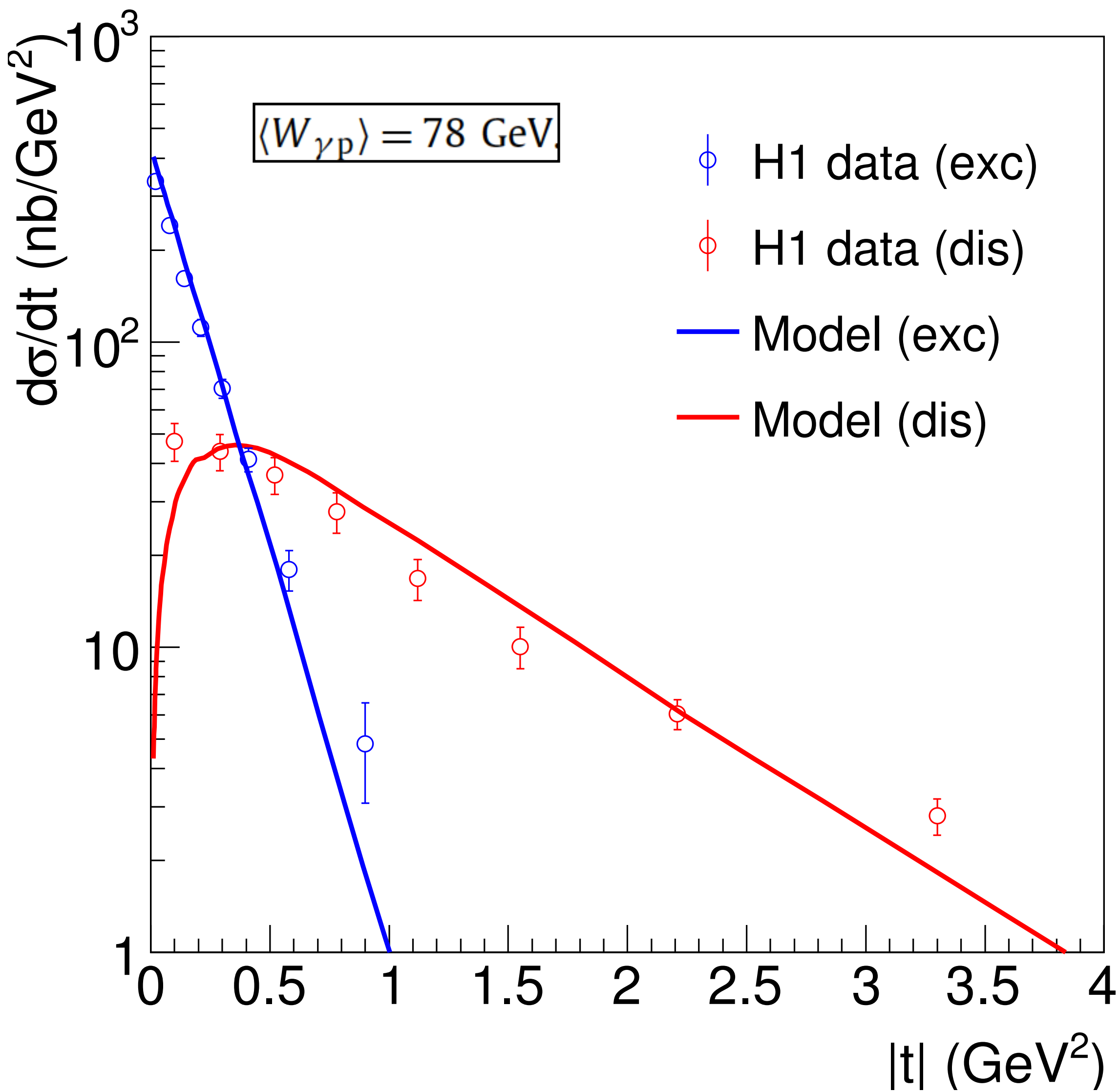
Comparison to J/ψ data

Čepila, JGC, Tapia , PLB 766 (2017) 186



Comparison to J/ ψ data

Čepila, JGC, Tapia , PLB 766 (2017) 186

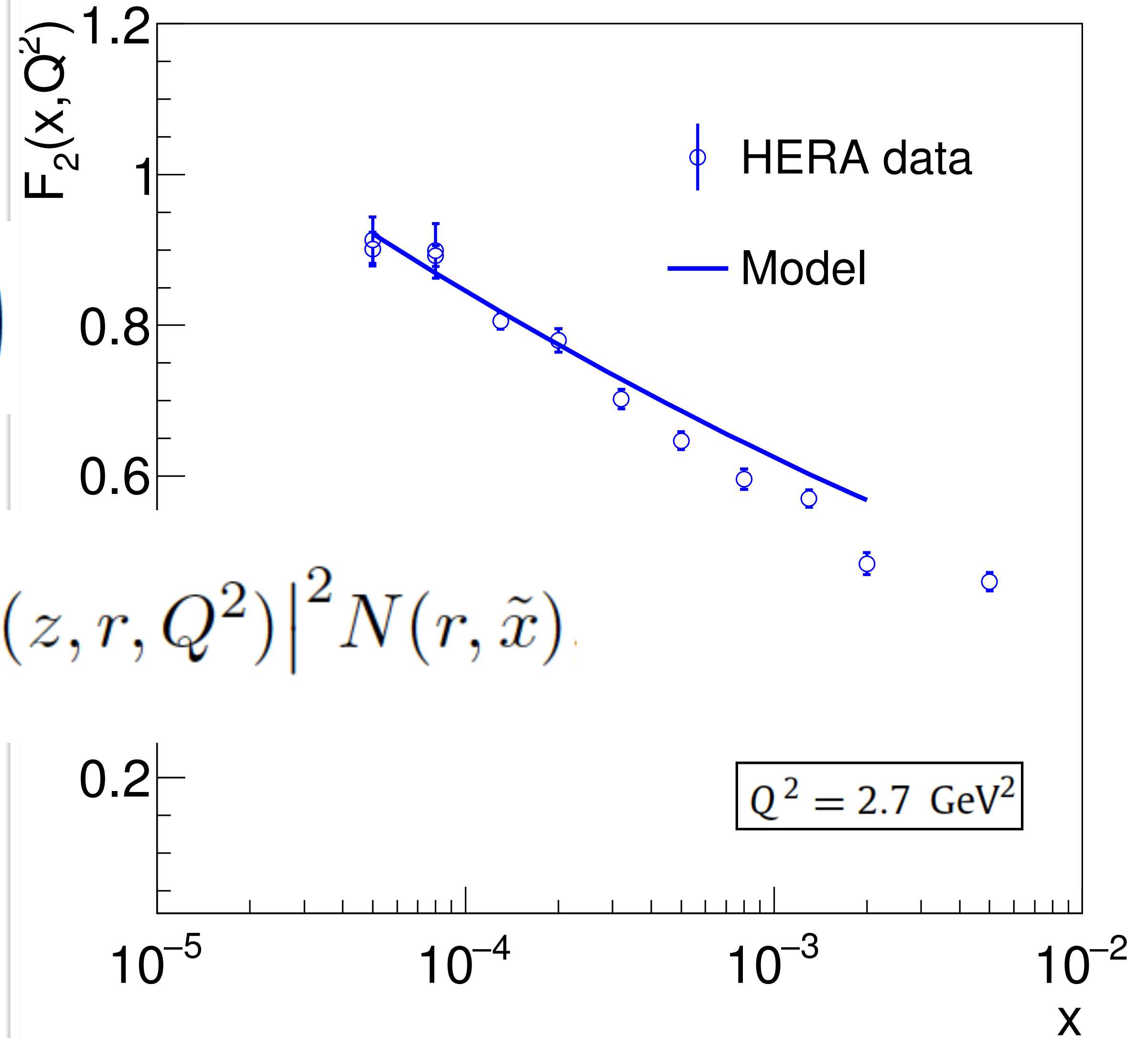


Comparison to inclusive data

Čepila, JGC, Tapia , PLB 766 (2017) 186

$$F_2(x, Q^2) = \frac{Q^2}{4\pi^2\alpha_{em}} \left(\sigma_T^{\gamma^*p}(x, Q^2) + \sigma_L^{\gamma^*p}(x, Q^2) \right)$$

$$\sigma_{T,L}^{\gamma^*p}(x, Q^2) = \sigma_0 \int d\vec{r} \int_0^1 dz \left| \Psi_{T,L}^{\gamma^* \rightarrow q\bar{q}}(z, r, Q^2) \right|^2 N(r, \tilde{x})$$

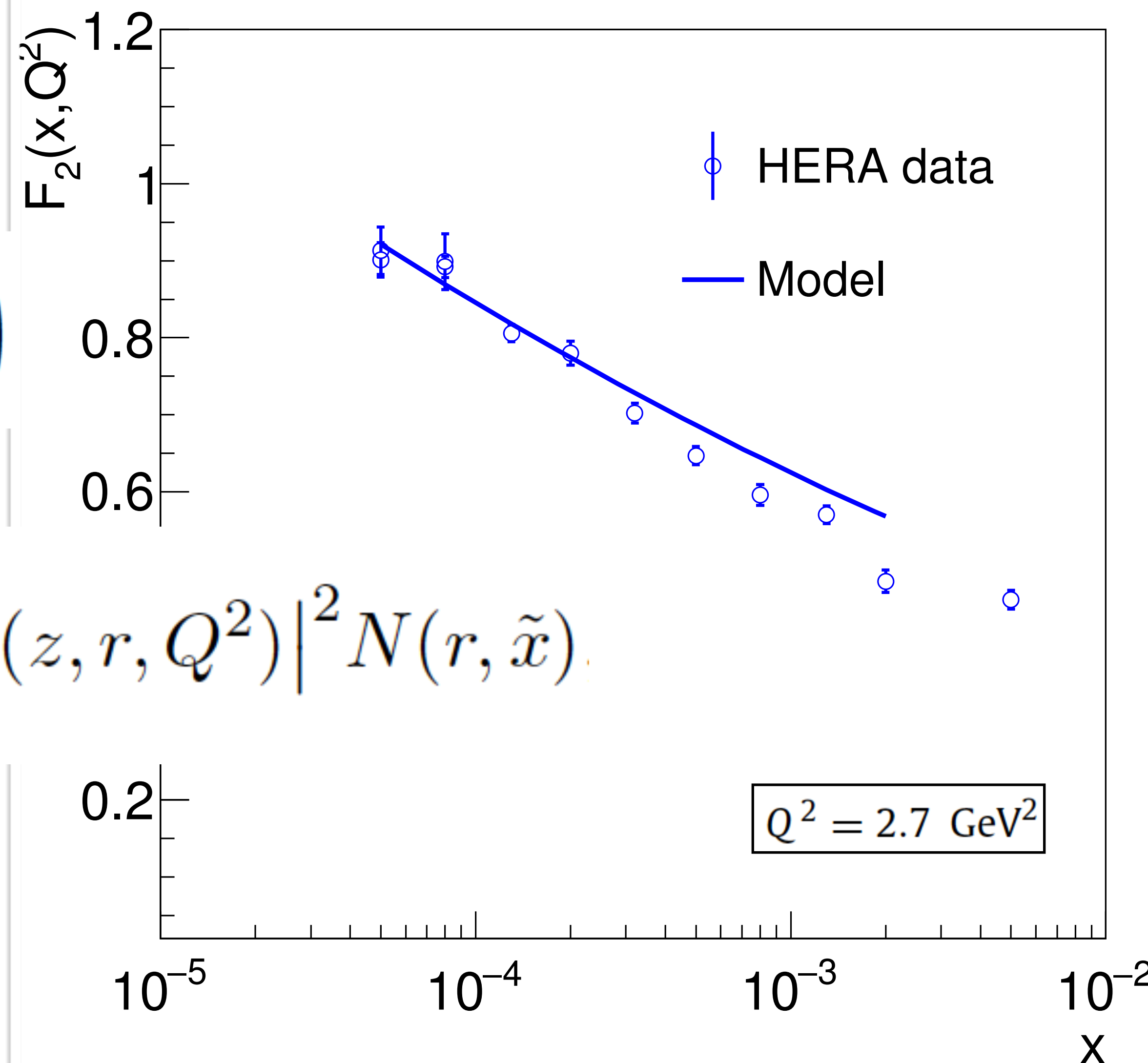


Comparison to inclusive data

Čepila, JGC, Tapia , PLB 766 (2017) 186

$$F_2(x, Q^2) = \frac{Q^2}{4\pi^2\alpha_{em}} \left(\sigma_T^{\gamma^*p}(x, Q^2) + \sigma_L^{\gamma^*p}(x, Q^2) \right)$$

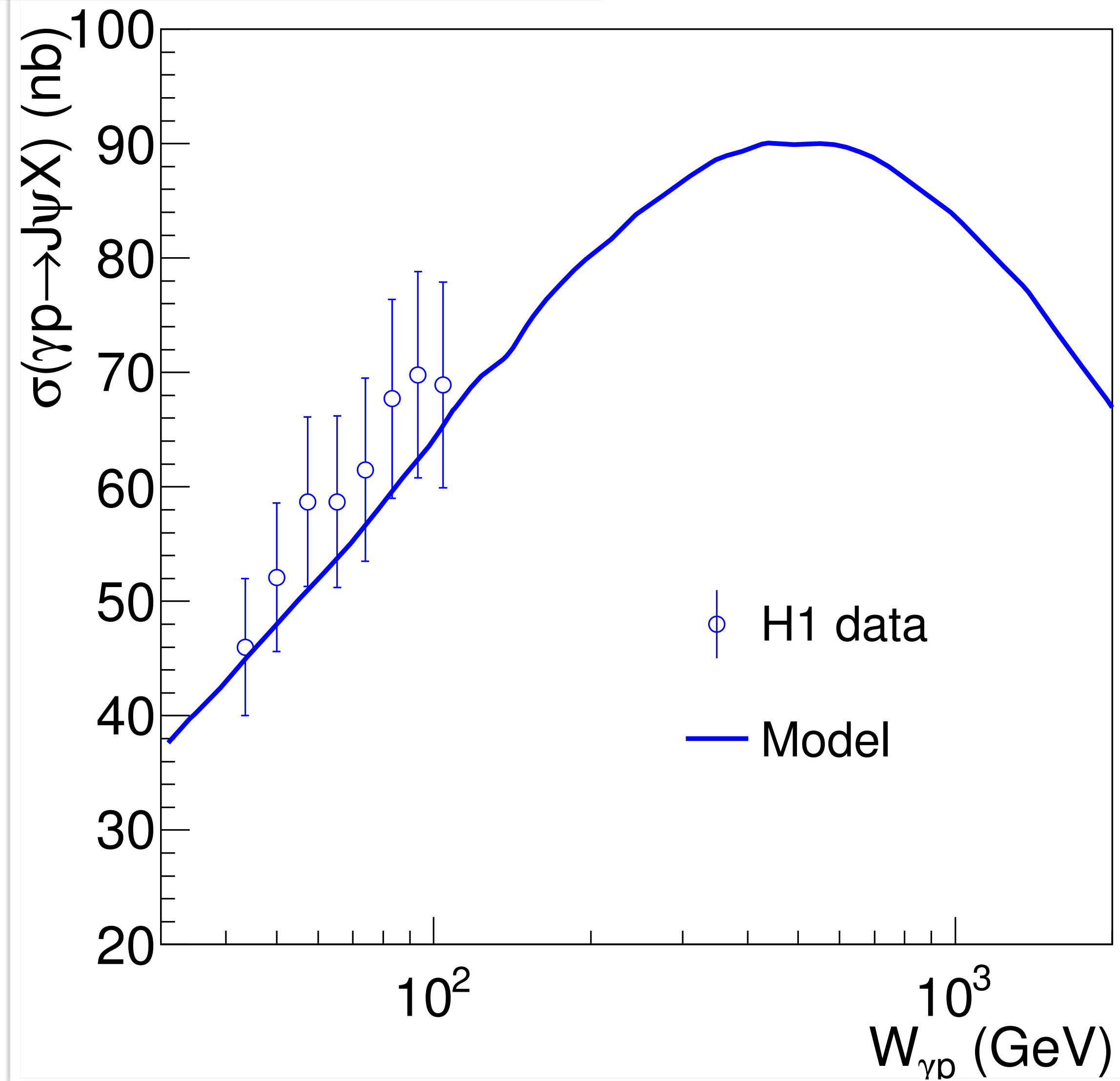
$$\sigma_{T,L}^{\gamma^*p}(x, Q^2) = \sigma_0 \int d\vec{r} \int_0^1 dz \left| \Psi_{T,L}^{\gamma^* \rightarrow q\bar{q}}(z, r, Q^2) \right|^2 N(r, \tilde{x})$$



Good description even though the model was developed for vector meson production.

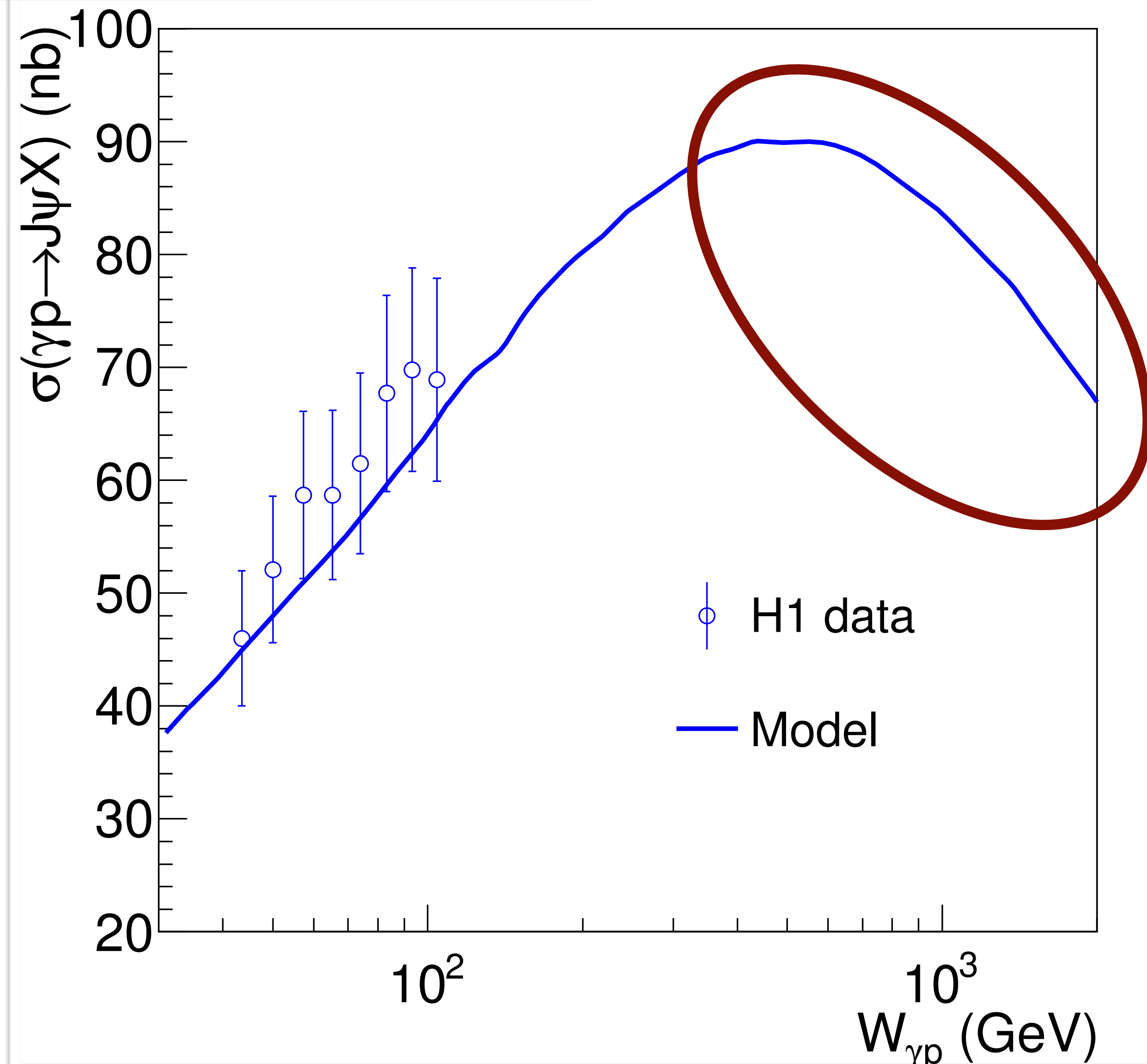
Prediction for the energy dependence of dissociative production

Čepila, JGC, Tapia, PLB 766 (2017) 186



Prediction for the energy dependence of dissociative production

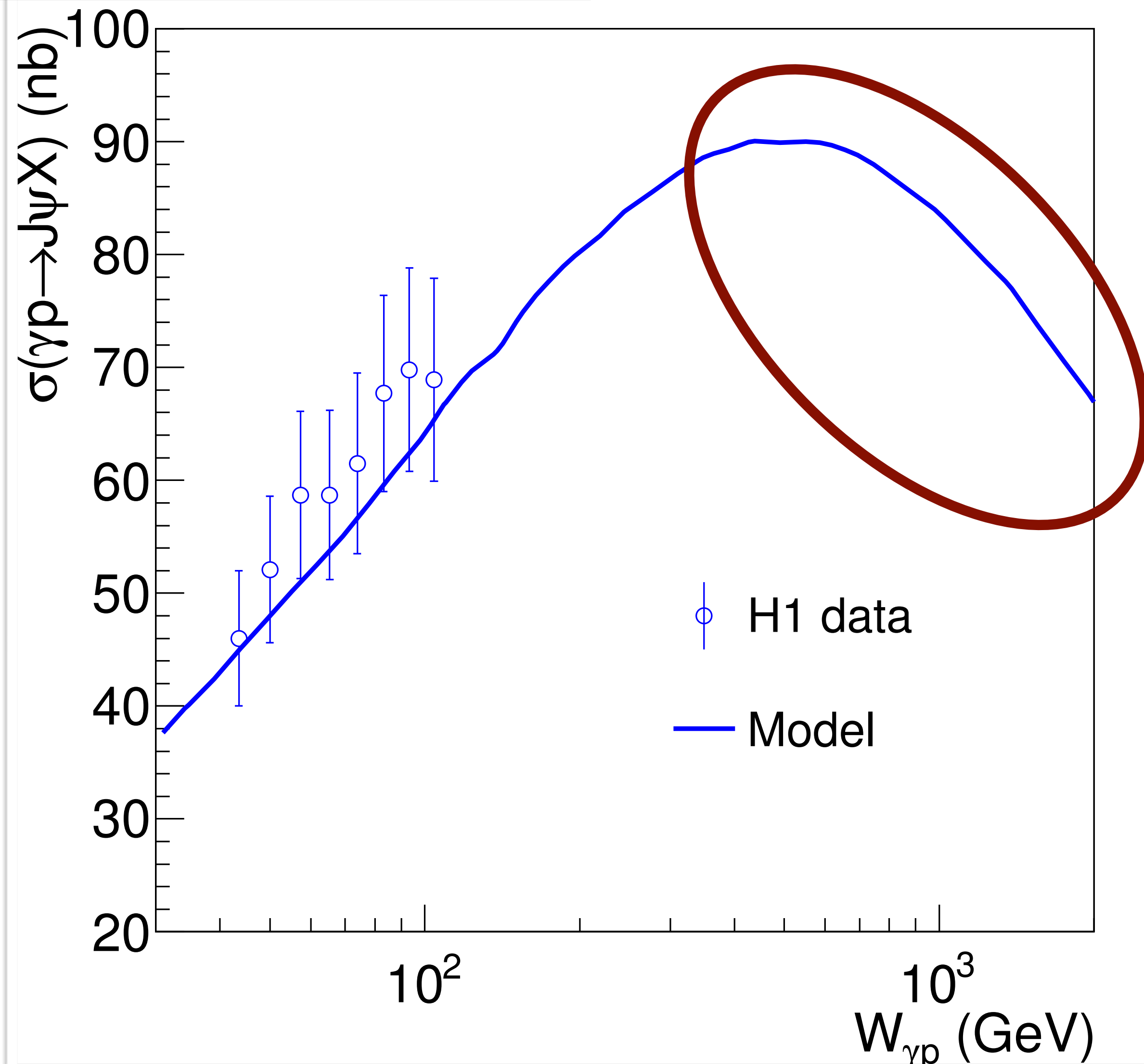
Čepila, JGC, Tapia, PLB 766 (2017) 186



- The model predicts an **striking signature** for saturation:
 - As the number of hot spot grows, the hot spots fill up the proton.
 - When saturation is reached, all configurations are very similar and the variance over configurations tends to zero.

Prediction for the energy dependence of dissociative production

Čepila, JGC, Tapia, PLB 766 (2017) 186



- The model predicts an **striking signature** for saturation:
 - As the number of hot spot grows, the hot spots fill up the proton.
 - When saturation is reached, all configurations are very similar and the variance over configurations tends to zero.

At the LHC we can measure J/ψ production accompanied by proton dissociation in this energy range!

News from J/ψ production in γPb collisions

Extension of the model to the case of nuclear targets

Glauber-Gribov approach:

$$\left(\frac{d\sigma_{dA}}{d\vec{b}}\right)_j = 2 \left[1 - \exp \left(-\frac{1}{2} \sigma_{dp}(x, r) T_A^j(\vec{b}) \right) \right],$$

Position of nucleons from a Woods-Saxon distribution,
position of hot spots as before.

Armesto, EPJC26 (2002) 35-43

Extension of the model to the case of nuclear targets

Glauber-Gribov approach:

$$\left(\frac{d\sigma_{dA}}{d\vec{b}}\right)_j = 2 \left[1 - \exp \left(-\frac{1}{2} \sigma_{dp}(x,r) T_A^j(\vec{b}) \right) \right],$$

Position of nucleons from a Woods-Saxon distribution, position of hot spots as before.

Armesto, EPJC26 (2002) 35-43

Nuclear saturation scale from geometric scaling arguments

$$\left(\frac{d\sigma_{dA}}{d\vec{b}}\right)_j = \sigma_0^A \left[1 - \exp \left(-r^2 Q_{A,s}^2(x)/4 \right) \right] T_A^j(\vec{b}).$$

$$Q_{s,A}^2(x) = Q_s^2(x) \left(\frac{A\pi R_p^2}{\pi R_A^2} \right)^{\frac{1}{\delta}},$$

Armesto, Salgado, Wiedemann, PRL94 (2005) 022002

Extension of the model to the case of nuclear targets

Glauber-Gribov approach:

$$\left(\frac{d\sigma_{dA}}{d\vec{b}}\right)_j = 2 \left[1 - \exp\left(-\frac{1}{2}\sigma_{dp}(x,r)T_A^j(\vec{b})\right) \right],$$

Position of nucleons from a Woods-Saxon distribution, position of hot spots as before.

Armesto, EPJC26 (2002) 35-43

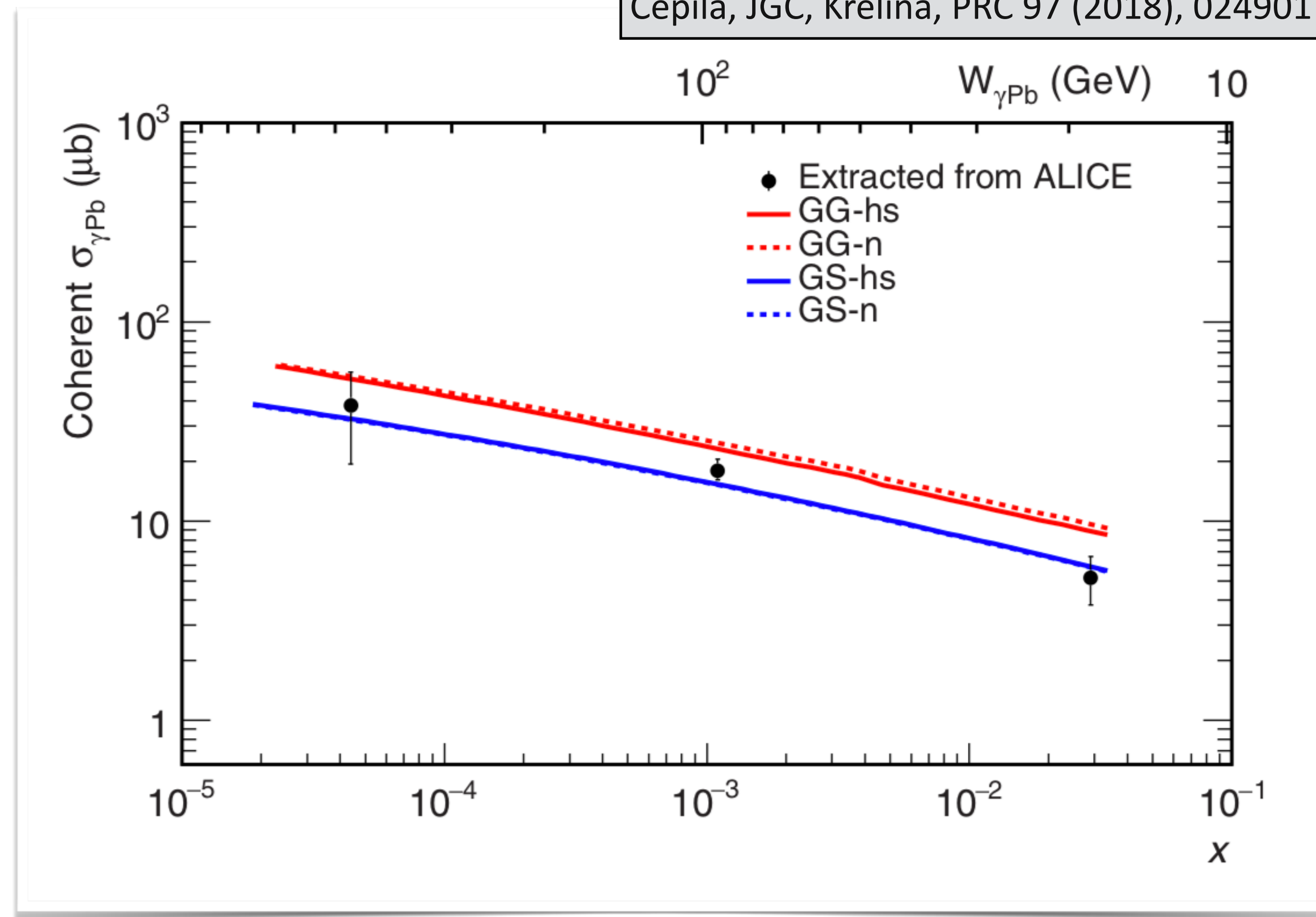
Nuclear saturation scale from geometric scaling arguments

$$\left(\frac{d\sigma_{dA}}{d\vec{b}}\right)_j = \sigma_0^A \left[1 - \exp\left(-r^2 Q_{A,s}^2(x)/4\right) \right] T_A^j(\vec{b}).$$

$$Q_{s,A}^2(x) = Q_s^2(x) \left(\frac{A\pi R_p^2}{\pi R_A^2} \right)^{\frac{1}{\delta}},$$

Armesto, Salgado, Wiedemann, PRL94 (2005) 022002

Čepila, JGC, Křelina, PRC 97 (2018), 024901



Good description of available data!

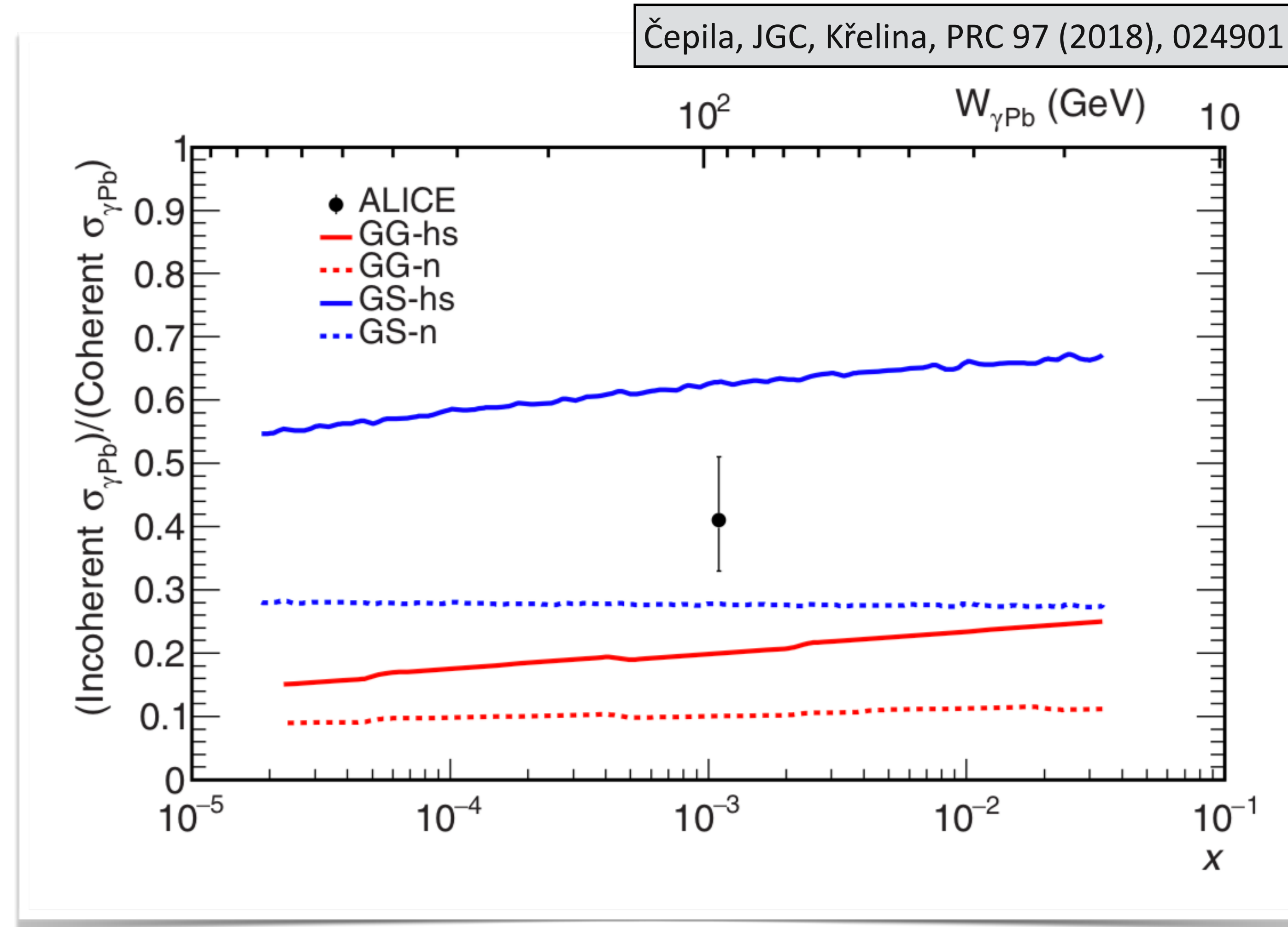
Ratio of incoherent to coherent cross sections

If the photon interact only with one nucleon in the nucleus, the process is called incoherent and the cross section is given by the variance over configurations as in the case for dissociative production.

Ratio of incoherent to coherent cross sections

If the photon interact only with one nucleon in the nucleus, the process is called incoherent and the cross section is given by the variance over configurations as in the case for dissociative production.

The energy dependence on the number of the subnuclear degrees of freedom produces and energy dependence on the ratio of incoherent to coherent cross section.



News from other vector mesons

Extension of the model to other vector mesons

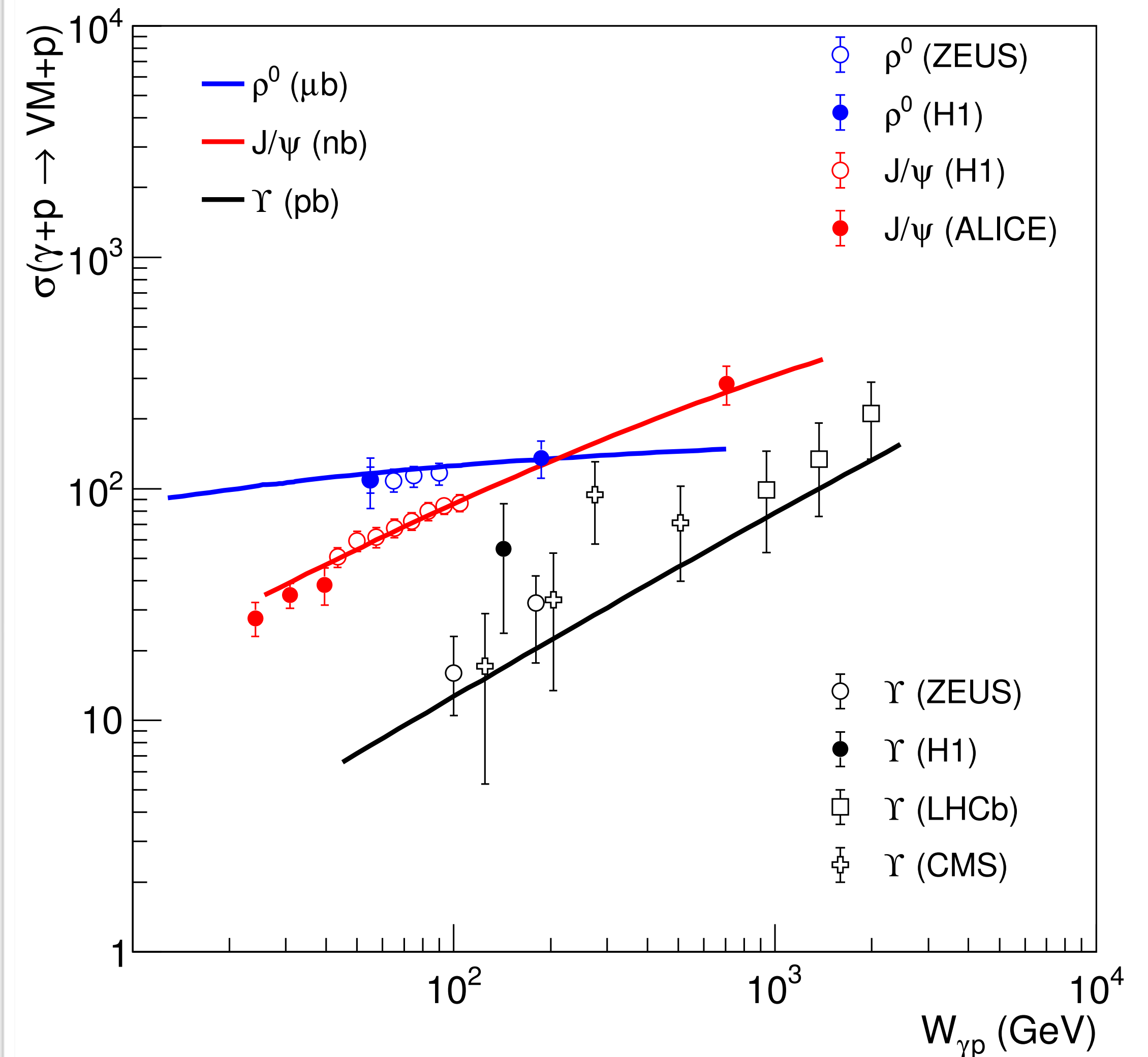
Only change needed is for the ρ^0 , where the positions of the hot spots within the proton are sampled from a Gaussian of width $B_p = 8 \text{ GeV}^{-2}$ instead of 4.7 GeV^{-2} .

Extension of the model to other vector mesons

Only change needed is for the ρ^0 , where the positions of the hot spots within the proton are sampled from a Gaussian of width $B_p = 8 \text{ GeV}^{-2}$ instead of 4.7 GeV^{-2} .

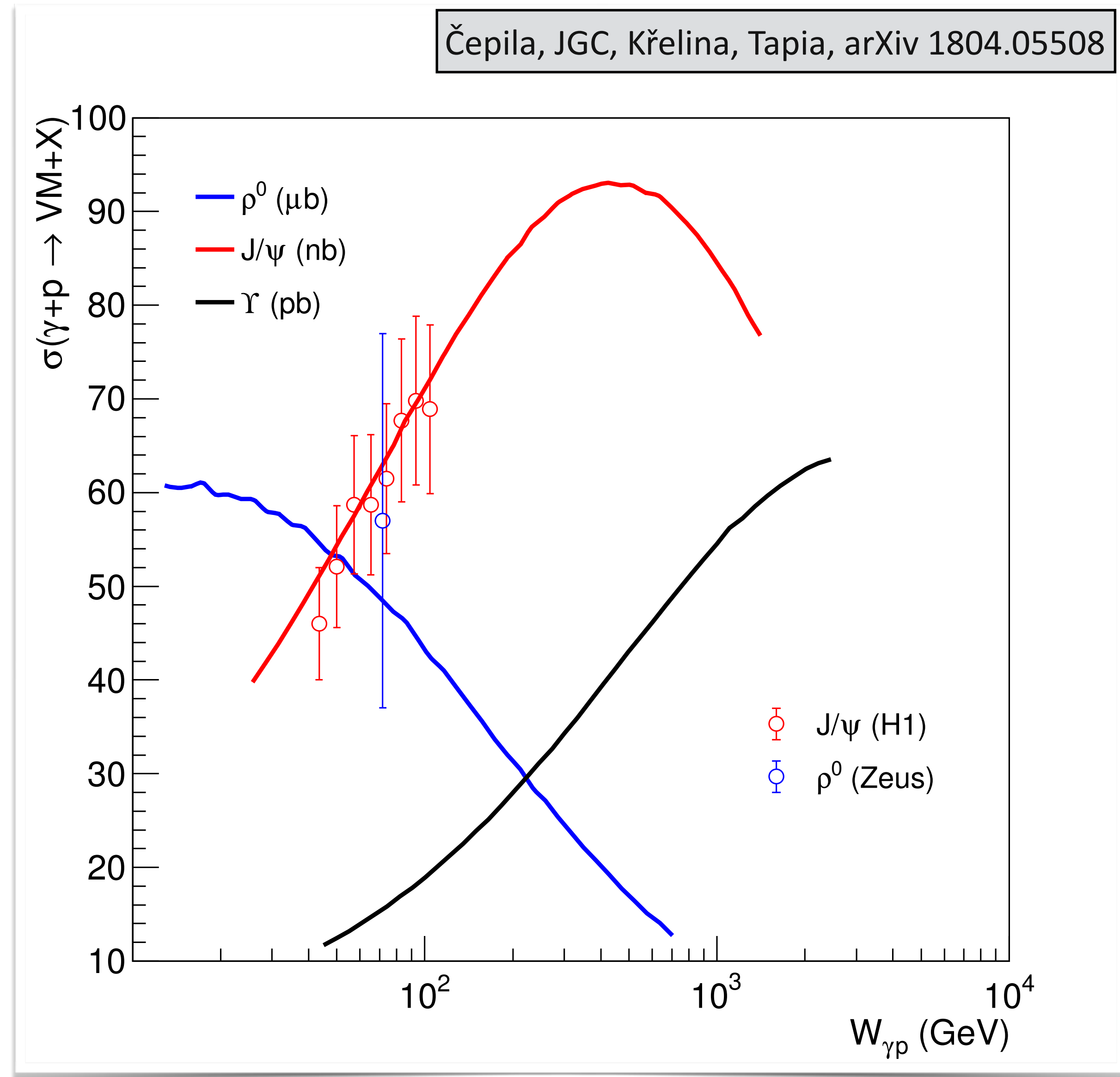
Good description of available data for exclusive production!

Čepila, JGC, Křelina, Tapia, arXiv 1804.05508



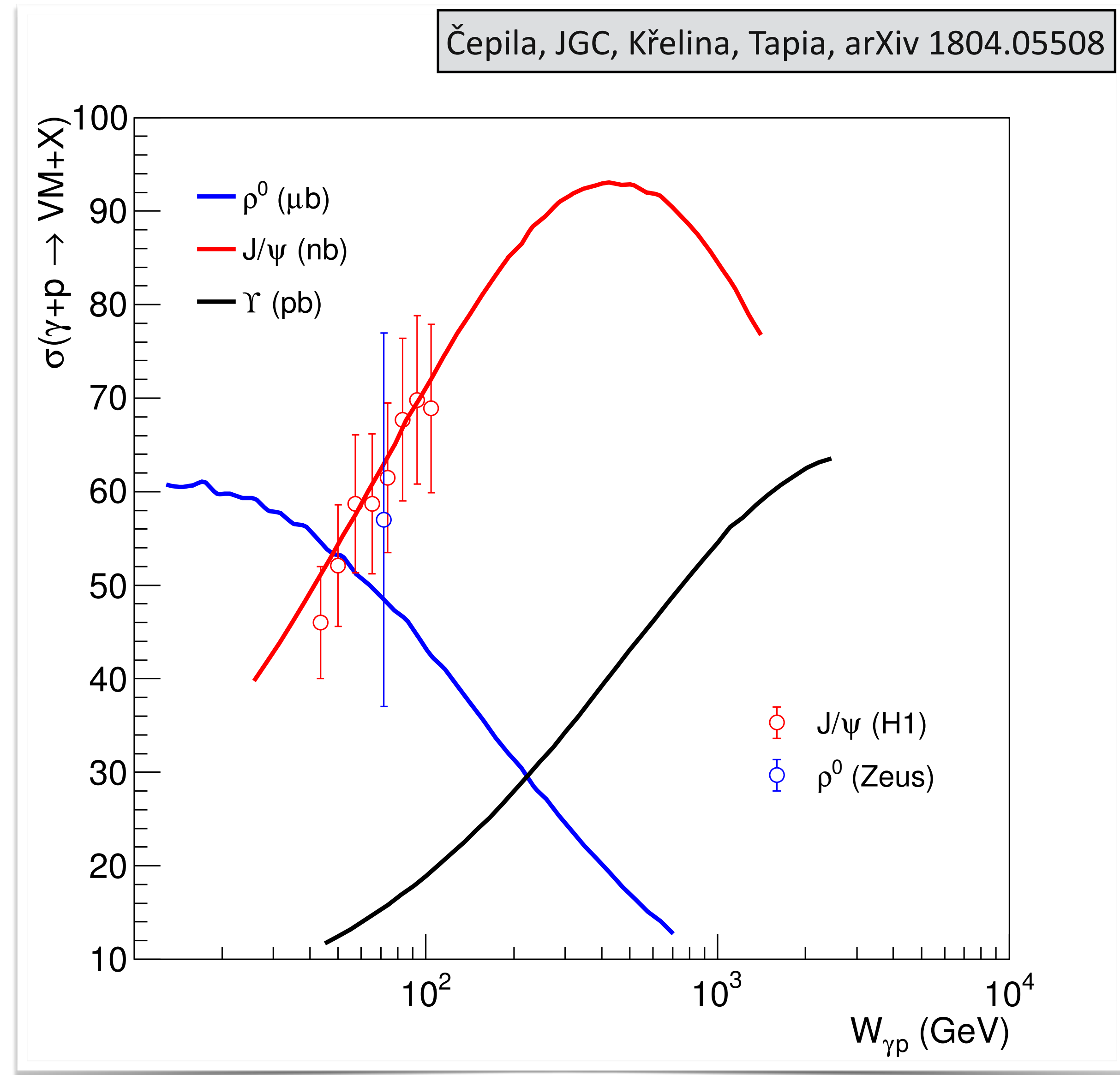
Extension of the model to other vector mesons: γp

- The position of the maximum of the dissociative cross section shifts with the mass of the vector meson.



Extension of the model to other vector mesons: γp

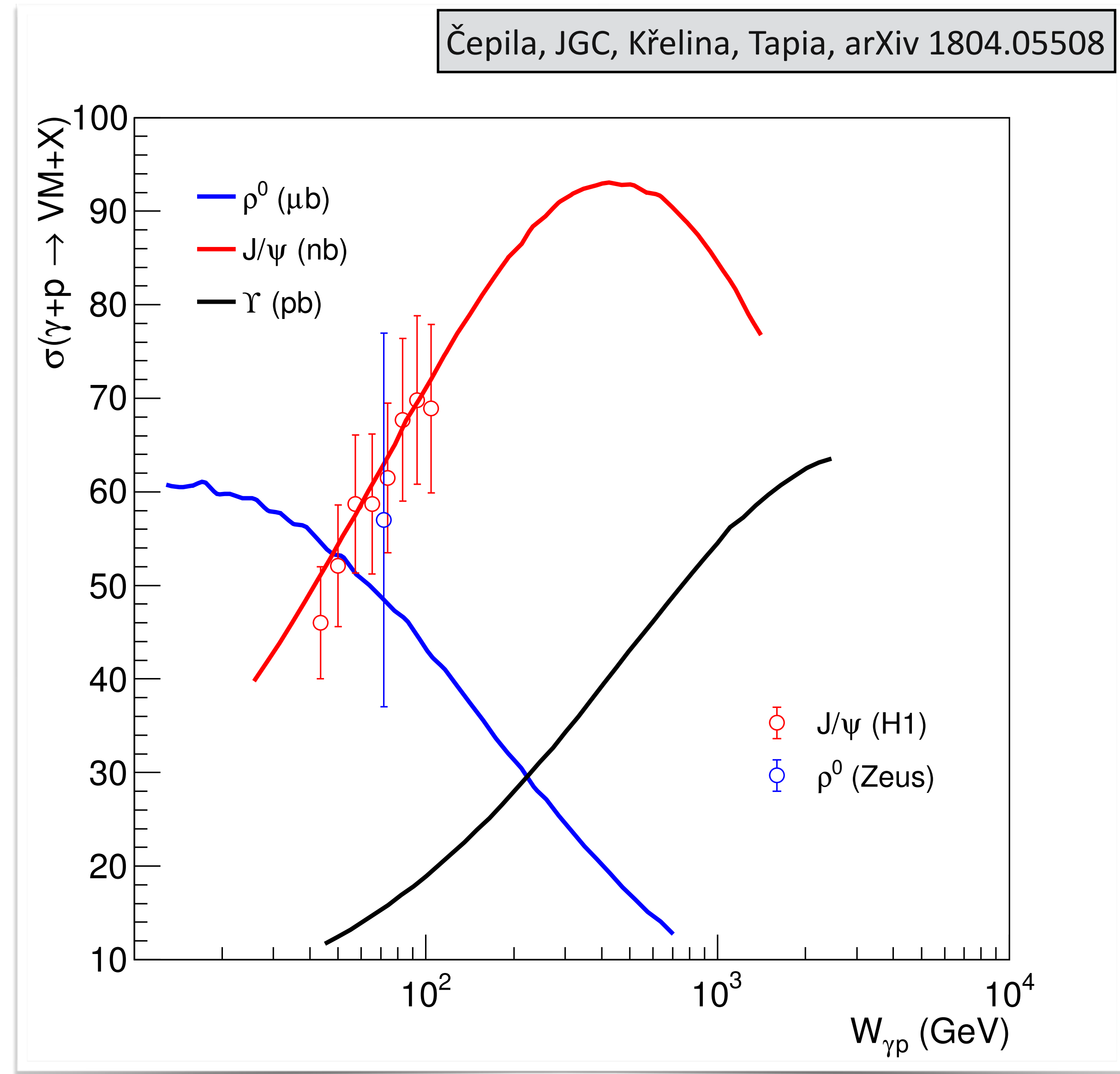
- The position of the maximum of the dissociative cross section shifts with the mass of the vector meson.
- The decrease of the cross section is given by the decrease in the variance over configurations; i.e., saturation.
- This shift on the maximum with the mass of the vector meson is related to the average dipole size from the convolution of the wave functions for the transitions of the photon to the diquark and from the diquark to vector meson.



Extension of the model to other vector mesons: γp

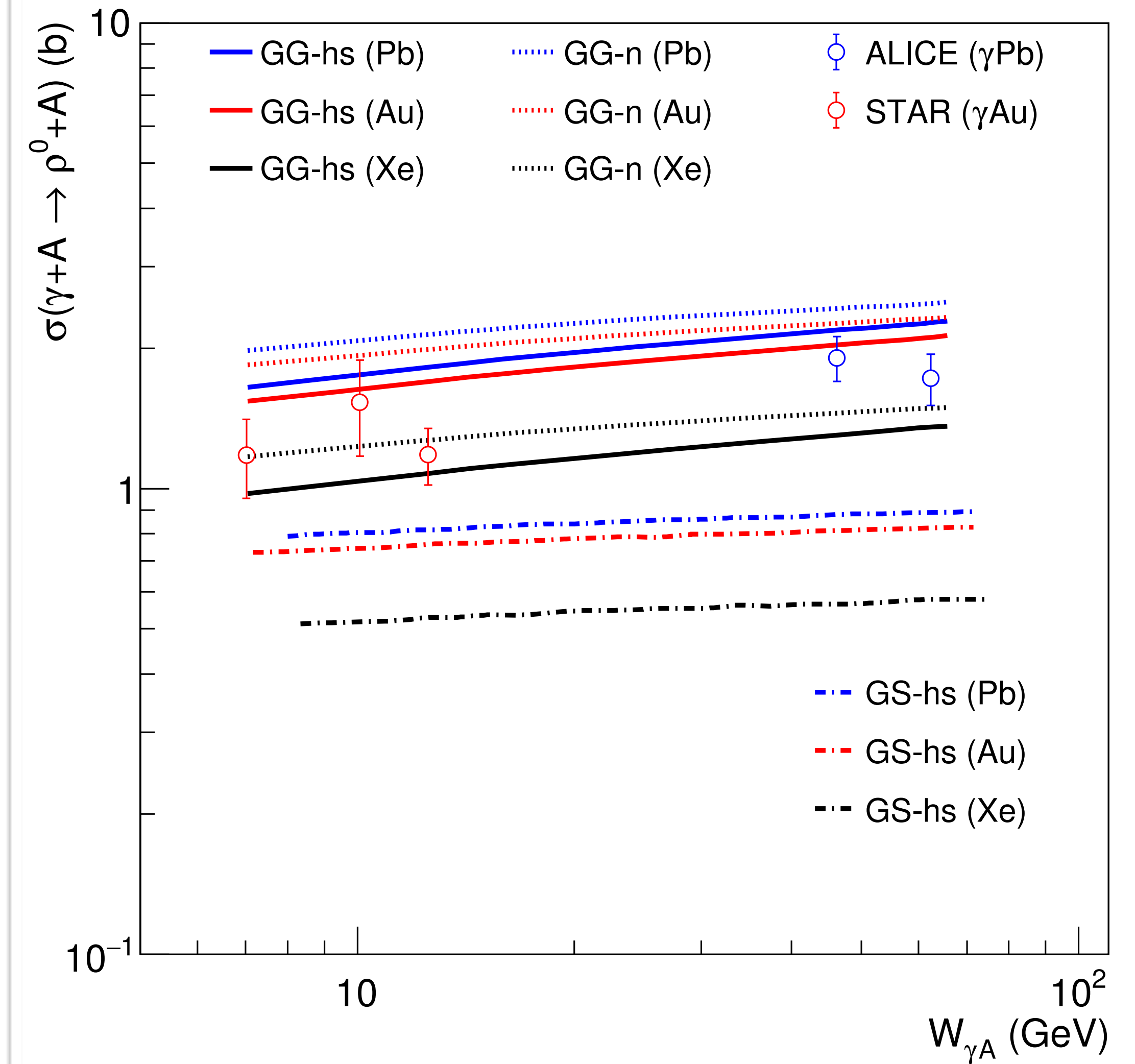
- The position of the maximum of the dissociative cross section shifts with the mass of the vector meson.
- The decrease of the cross section is given by the decrease in the variance over configurations; i.e., saturation.
- This shift on the maximum with the mass of the vector meson is related to the average dipole size from the convolution of the wave functions for the transitions of the photon to the diquark and from the diquark to vector meson.

Measuring at the LHC all three vector meson would provide a new handle to look for saturation effects.



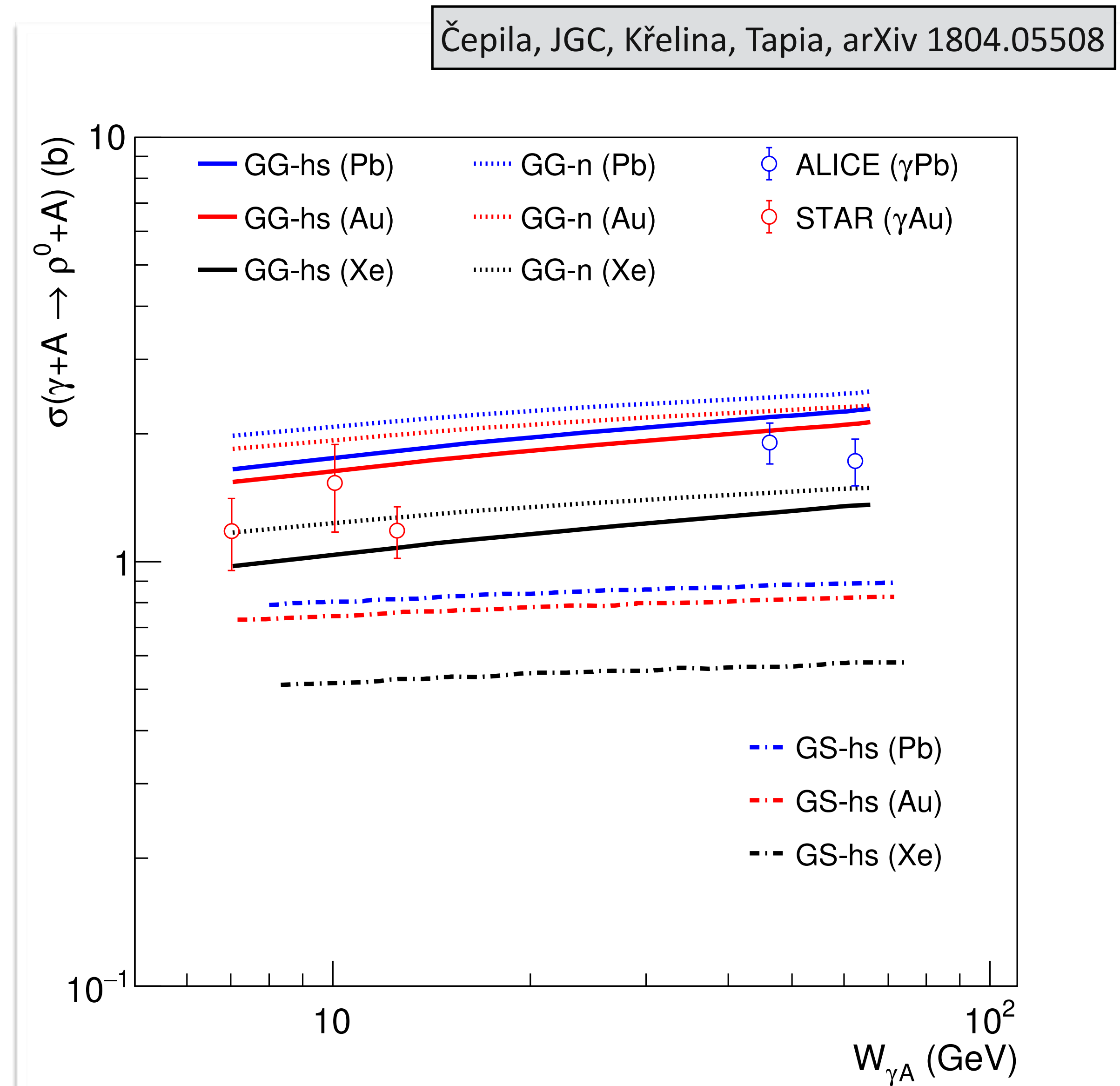
Extension of the model to other vector mesons: γ Pb

Čepila, JGC, Křelina, Tapia, arXiv 1804.05508



Extension of the model to other vector mesons: γ Pb

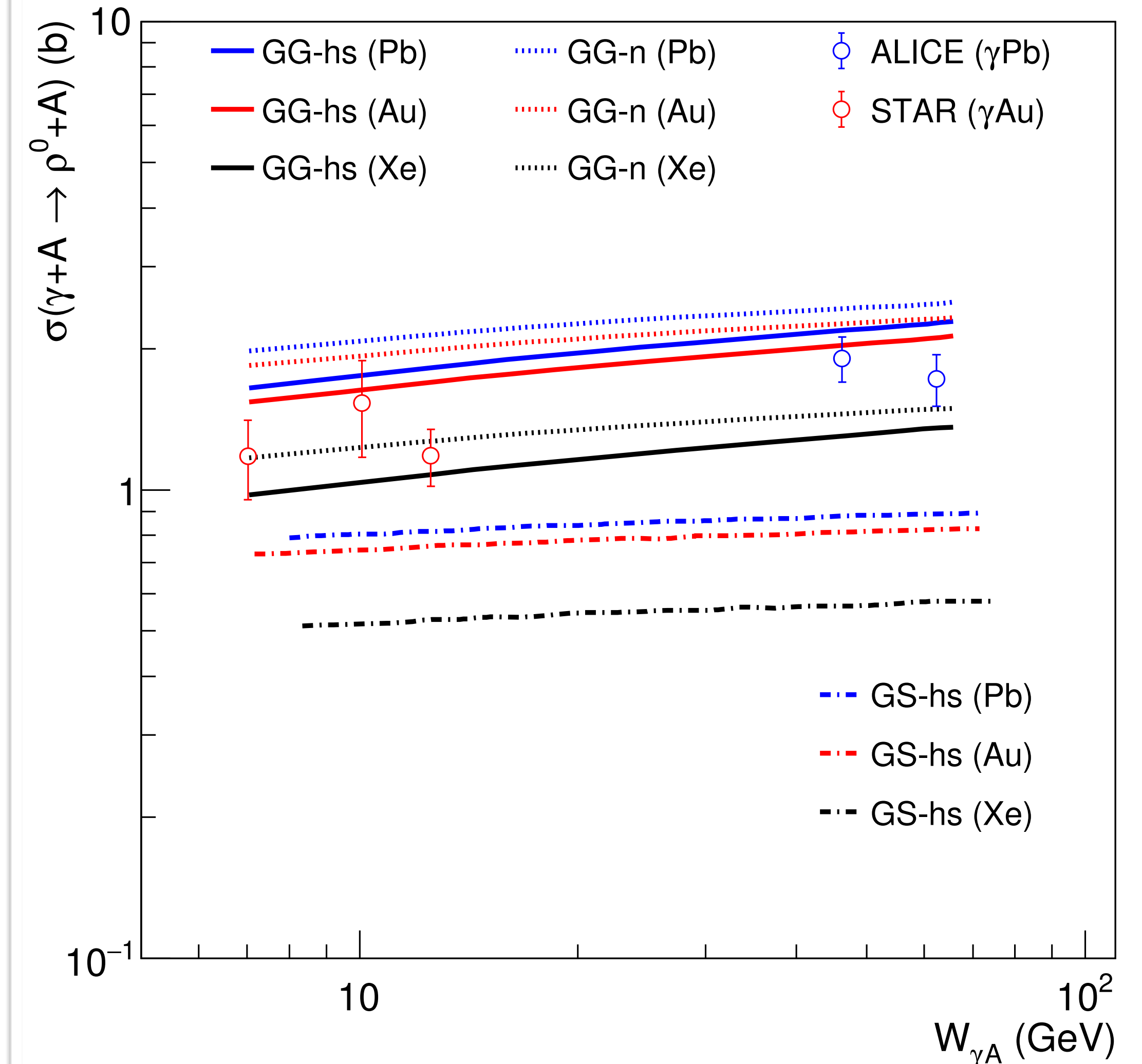
- The model based on geometric scaling ideas predicts a cross section for coherent production of ρ^0 about a factor of 2 smaller than data.



Extension of the model to other vector mesons: γ Pb

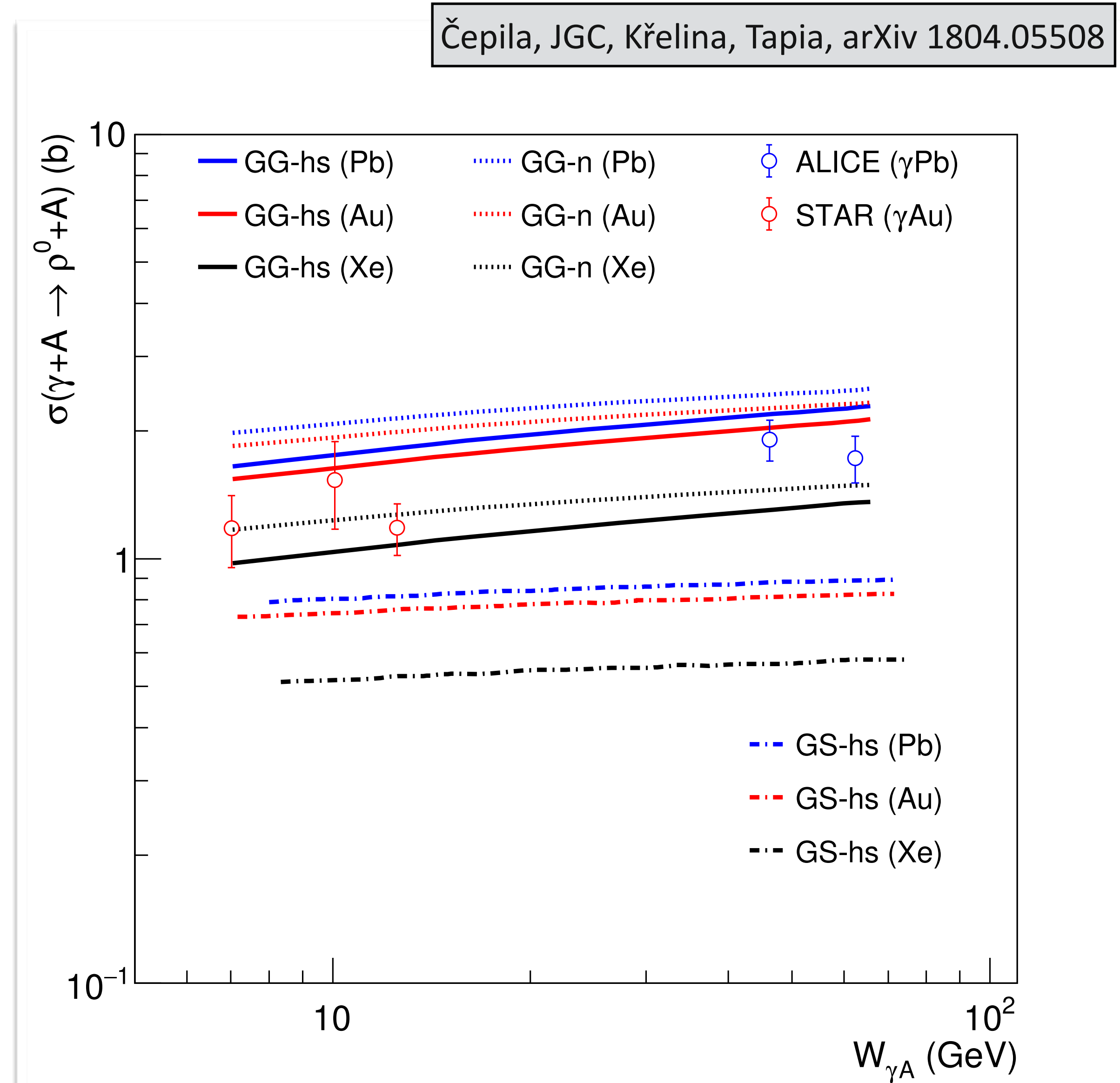
- The model based on geometric scaling ideas predicts a cross section for coherent production of ρ^0 about a factor of 2 smaller than data.
- The model based on Gribov-Glauber ideas overshoots data by a bit more than one sigma.

Čepila, JGC, Křelina, Tapia, arXiv 1804.05508



Extension of the model to other vector mesons: γ Pb

- The model based on geometric scaling ideas predicts a cross section for coherent production of ρ^0 about a factor of 2 smaller than data.
- The model based on Gribov-Glauber ideas overshoots data by a bit more than one sigma.
- In this model, there is a **difference** in the energy evolution of the coherent cross section **when adding subnucleon degrees of freedom**.



Summary and outlook

Summary and outlook

- News from J/ψ production in γp collisions:
 - The energy dependence of dissociative J/ψ photoproduction provides a striking signature for saturation.
- News from J/ψ production in γPb collisions:
 - Fluctuations of subnuclear degrees of freedom also leave an imprint in the photoproduction of J/ψ off nuclear targets.
- News from other vector mesons:
 - The mass dependence of vector meson photoproduction provides a new handle in the search for saturation effects.

Čepila, JGC, Tapia , PLB 766 (2017) 186

Čepila, JGC, Křelina, PRC 97 (2018), 024901

Čepila, JGC, Křelina, Tapia, arXiv 1804.05508

Eagerly awaiting new data on photoproduction of vector mesons off protons and off nuclei!